Chiral C_1-Symmetric Group 4 Metallocenes as Catalysts for Stereoregular α-Olefin Polymerization. Metal, Ancillary Ligand, and Counteranion Effects

Michael A. Giardello, Moris S. Eisen, Charlotte L. Stern, and Tobin J. Marks*

Contribution from the Department of Chemistry, Northwestern University, Evanston, Illinois 60208-3113

Received May 19, 1995[⊗]

Abstract: This contribution reports the synthesis and activity as precatalysts for stereoselective propylene polymerization of several chiral non-C_2 symmetric zirconocene and hafnocene complexes, (*R*)- and (*S*)-$Me_2Si(Me_4C_5)(C_5H_3R^*)MR_2$ (R = Cl(**2**) or Me(**3**)) where R* = (1*R*,2*S*,5*R*)-*trans*-5-methyl-*cis*-2-(2-propyl)cyclohexyl ((−)-menthyl; M = Zr, (**a**) and M = Hf, (**b**)) and (1*S*,2*S*,5*R*)-*trans*-5-methyl-*cis*-2-(2-propyl)cyclohexyl ((+)-neomenthyl; M = Zr (**c**)). Metallocene dichlorides were prepared from MCl_4 and $Li_2Me_2Si(Me_4C_5)(C_5H_3R^*)$ and converted to the corresponding dimethyl complexes with MeLi·LiBr. All complexes were characterized by standard techniques, with absolute configuration established by circular dichroism and X-ray diffraction. For the (*R*) − R* = (−)-menthyldichloro complex (**2a**): space group = $P2_12_12_1$; a = 9.404(2), b = 9.817(3), c = 28.684(7) Å(−120 °C), Z = 4; R(F) = 0.056, R_w(F) = 0.061 for 2025 reflections having $I > 3\sigma(I)$. For the (*R*) − R* = (−)-menthyldimethyl complex (**3a**): space group = $P2_1$; a = 9.501(3), b = 9.394(3), c = 15.565(3) Å, β = 103.76(2)°(−120 °C), Z = 2; R(F) = 0.037, R_w(F) = 0.039 for 1528 reflections having $I > 3\sigma(I)$. Reaction of either (*R*)-**3a** or (*R*)-**3b** with $B(C_6F_5)_3$ in toluene yields two spectroscopically discernible methyl cations. The temperature dependence of the ion-pair equilibrium constant in toluene yields ΔH = −0.7(1) kcal/mol and ΔS = −3.1(1) eu for (*R*)-**3a** and ΔH = 0.14(3) kcal/mol and ΔS = −3.1(1) for (*R*)-**3b**. "Cationic" propylene polymerization catalysts were generated from **2** + methylalumoxane or **3** + methylalumoxane, $B(C_6F_5)_3$, $Ph_3C^+B(C_6F_5)_4^-$, or $HN(^nBu_3)^+B(C_6F_5)_4^-$. Polymerization activities, stereoregularities, and polymer molecular weights are strongly dependent on cocatalyst identities and concentrations, suggesting strong, structure-sensitive ion-pairing effects. Polypropylene isotacticities as high as 95% mmmm pentad content are observed, with stereoregularity increasing and polymerization activity falling with decreasing reaction temperature.

Introduction

The stereoregular polymerization and hydrooligomerization of α-olefins[1−6] mediated by "cationic" [7] chiral group 4 metallocenes has been studied intensely in recent years. Ewen first demonstrated their efficacy when he employed C_2-symmetric ethanobridged-indenyl-titanocene/MAO system **A** as the first example of an effective homogeneous isospecific propylene

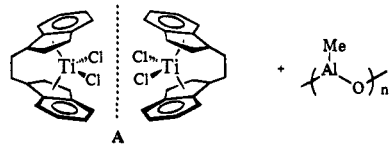

A

polymerization catalyst.[2e] Ewen demonstrated that titanocene

[⊗] Abstract published in *Advance ACS Abstracts*, October 15, 1995.

(1) For an excellent review of chiral metallocene-mediated stereospecific olefin polymerization, see: Brintzinger, H. H.; Fischer, D.; Mülhaupt, R.; Rieger, B.; Waymouth, R. M. *Angew. Chem.* **1995**, *34*, 1143−1170, and references therein.

(2) For representative recent isotactic polypropylene work see ref 1 and (a) Spaleck, W.; Küber, F.; Winter, A.; Rohrmann, J.; Bachmann, B.; Antberg, M.; Dolle, V.; Paulus, E. F. *Organometallics* **1994**, *13*, 954−963. (b) Razavi, A.; Atwood, J. L. *J. Am. Chem. Soc.* **1993**, *115*, 7529−7530. (c) Spaleck, W.; Antberg, M.; Rohrmann, J.; Winter, A.; Bachmann, B.; Kiprof, P.; Behm, J.; Herrmann, W. A. *Angew. Chem., Int. Ed. Engl.* **1992**, *31*, 1347−1349. (d) Chien, J. C. W.; Tsai, W. M.; Rausch, M. D. *J. Am. Chem. Soc.* **1991**, *113*, 8570−8571. (e) Ewen, J. A. *J. Am. Chem. Soc.* **1984**, *106*, 6355−6364.

(3) For representative recent syndiotactic polypropylene work see ref 1 and (a) Razavi, A.; Atwood, J. L. *J. Organomet. Chem.* **1993**, *459*, 117−123. (b) Bochmann, M.; Lancaster, S. J. *Makromol. Chem., Rapid Commun.* **1993**, *14*, 807−811. (c) Ewen, J. A.; Elder, M. J.; Jones, R. L.; Haspeslagh, L.; Atwood, J. L. *Makromol. Chem., Macromol. Symp.* **1991**, *48/49*, 253−295. (d) Ewen, J. A.; Elder, M. J.; Jones, R. L.; Curtis, S.; Cheng, H. N. In *Catalytic Olefin Polymerization*; Keii, T., Soga, K., Eds.; Elsevier: New York, 1990; pp 439−482.

(4) For representative recent thermoplastic elastomer work see ref 1 and (a) Coates, G. W.; Waymouth, R. M. *Science* **1995**, *267*, 217−219. (b) Llinas, G. H.; Dong, S. H.; Mallin, D. T.; Rausch, M. D.; Lin, Y. G.; Winter, H. H.; Chien, J. C. W. *Macromolecules* **1992** *25*, 1242−1253. (c) Chien, J. C. W.; Llinas, G. H.; Rausch, M. D.; Lin, G. Y.; Winter, H. H. *J. Am. Chem. Soc.* **1991**, *113*, 8569−8570.

(5) Representative recent theoretical studies: (a) Yoshida, T.; Koga, N.; Morokuma, K. *Organometallics* **1995**, *14*, 746−758. (b) Woo, T. K.; Fan, L.; Ziegler, T. *Organometallics* **1994**, *13*, 2252−2261. (c) Bierwagen, E. P.; Bercaw, J. E.; Goddard, W. A. *J. Am. Chem. Soc.* **1994**, *116*, 1481−1489. (d) Guerra, G.; Cavallo, L.; Moscardi, G.; Vacatello, M.; Corradini, P. *J. Am. Chem. Soc.* **1994**, *116*, 2988−2995. (e) Meier, R.; Van Doremaele, G. H. J.; Iarlori, S.; Buda, F. *J. Am. Chem. Soc.* **1994**, *116*, 7274−7281. (f) Hart, J. R.; Rappé, A. K. *J. Am. Chem. Soc.* **1993**, *115*, 6159−6164. (g) Castonguay, L. A.; Rappé, A. K. *J. Am. Chem. Soc.* **1992**, *114*, 5832−5842. (h) Hortmann, K.; Brintzinger, H. H. *New J. Chem.* **1992**, *16*, 51−55.

(6) (a) Kaminsky, W.; Ahlers, A.; Möller-Lindenhof, N. *Angew. Chem., Int. Ed. Engl.* **1989**, *28*, 1216−1218. (b) Waymouth, R.; Pino, P. *J. Am. Chem. Soc.* **1990**, *112*, 4911−4914.

(7) (a) Möhring, P. C.; Coville, N. J. *J. Organomet. Chem.* **1994**, *479*, 1−29, and references therein. (b) Kaminsky, W. *Catalysis Today* **1994**, *20*, 257−271, and references therein. (c) Jordan, R. F. *Adv. Organomet. Chem.* **1991**, *32*, 325−387, and references therein. (d) Marks, T. J. *Acc. Chem. Res.* **1992**, *25*, 57−65, and references therein. (e) Deck, P. A.; Marks, T. J. *J. Am. Chem. Soc.* **1995**, *117*, 6128−6129. (f) Yang, X.; Stern, C.; Marks, T. J. *J. Am. Chem. Soc.* **1994**, *116*, 10015−10031. (g) Sishta, C.; Hathorn, R. M.; Marks, T. J. *J. Am. Chem. Soc.* **1992**, *114*, 1112−1114. (h) Bochmann, M.; Jaggar, A. J. *J. Organomet. Chem.* **1992**, *424*, C5−C7, and references therein. (i) Hlatky, G. G.; Eckman, R. R.; Turner, H. W. *Organometallics* **1992**, *11*, 1413−1416, and references therein. (j) Horton, A. D.; Orpen, A. G. *Organometallics* **1991**, *10*, 3910−3918, and references therein. (k) Eisch, J. J.; Caldwell, K. R.; Werner, S.; Krüger, C. *Organometallics* **1991**, *10*, 3417−3419, and references therein.

0002-7863/95/1517-12114$09.00/0

diphenyl also afforded isotactic polypropylene, but having a different microstructure. The former polymer has microstructure **B** resulting from enantiomorphic site-control, while the latter has microstructure **C** arising from chain-end-control. Subse-

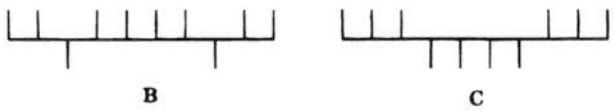

B **C**

quently, Ewen demonstrated that predominantly syndiotactic polypropylene **D** was produced when C_s-symmetric metallocene/MAO co-catalyst systems **E** were used.[3]

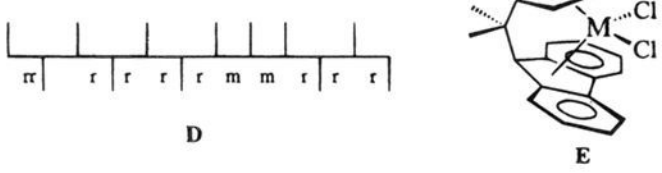

D **E**

Since these discoveries, there have been many metallocene-based systems developed for isospecific propylene polymerization.[1] With few exceptions,[4,8] these studies have been largely limited to ring-bridged bis(indenyl) and bis(tetrahydroindenyl) group 4 complexes and other axially symmetric metallocenes. In the course of group 4 complex synthesis, these ligand systems generally produce substantial quantities of unwanted "meso" metallocene **F**, with desired "racemate" **G** obtained only after nontrivial separation processes.[9] Furthermore, if a single antipode of **G** is desired, additional derivatization/separation steps are required.[10] In an effort to further explore the utility

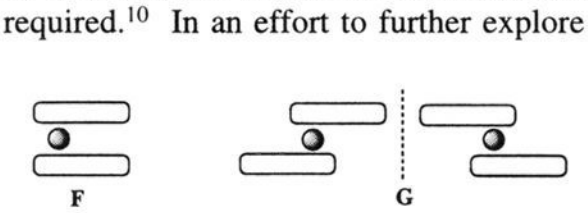

F **G**

and stereodifferentiating capacity of first-generation C_1-symmetric chiral ligand systems such as **H** and **I**, designed for asymmetric organolanthanide catalysis,[11] we developed a high yield route to chiral group 4 metallocenes.[12] These metallocenes, when combined with a variety of cation-forming co-catalysts, are shown in the present contribution to be highly active ethylene and isospecific propylene polymerization catalysts. Significant and informative counteranion effects are

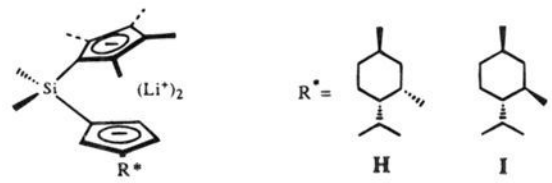

H **I**

observed which offer additional control of polymer microstructure and molecular weight.

Experimental Section

Materials and Methods. All manipulations of air-sensitive materials were performed with rigorous exclusion of oxygen and moisture in flamed Schlenk-type glassware on a dual manifold Schlenk line, interfaced to a high vacuum (10^{-6} Torr) line, or in a nitrogen-filled Vacuum Atmospheres glovebox with a high capacity recirculator (1−2 ppm O_2). Argon (Matheson, prepurified), nitrogen (Matheson, prepurified), and propylene (Matheson, polymerization grade) were purified by passage through a MnO/vermiculite oxygen-removal column and an activated Davison 4 Å molecular sieve column, followed by passage over MnO/silica.[13] Ether solvents were purified by distillation from Na/K alloy/benzophenone ketyl. Hydrocarbon solvents (toluene and pentane) were distilled under nitrogen from Na/K alloy. All solvents for vacuum line manipulations were stored *in vacuo* over Na/K alloy in resealable bulbs. Deuterated solvents were obtained from Cambridge Isotope Laboratories (all 99 + atom % D) and were freeze−pump−thaw degassed. Non-halogenated solvents were dried over Na/K alloy, and halogenated solvents were dried over P_2O_5 and stored over activated Davidson 4 Å molecular sieves. $ZrCl_4$ and $HfCl_4$ (Aldrich 99.99%) were used without further purification. Chiral ligand reagents Li_2Me_2SiCp''[(−)-menthylCp] and Li_2Me_2SiCp''[(+)-neomenthylCp] were prepared as previously described.[11a] $B(C_6F_5)_3$,[14] *n*-$Bu_3NHB(C_6F_5)_4$,[15] and $Ph_3CB(C_6F_5)_4$[2d] were prepared according to literature procedures. Solid methylalumoxane was obtained by slow removal of solvent *in vacuo* (10^{-6} Torr) at 25 °C from a solution of MAO (Schering, 20 wt % solution in toluene). Prolonged evacuation (12−16 h) of the residual solids removed a majority of the $AlMe_3$.

Physical and Analytical Measurements. NMR spectra were recorded on either Varian VXR 300 (FT, 300 MHz, ^{1}H; 75 MHz, ^{13}C), Varian XL-400 (FT, 400 MHz, ^{1}H; 376 MHz, ^{19}F; 100 MHz, ^{13}C), or Bruker AMX 600 (FT, 600.14 MHz, ^{1}H; MHz, ^{13}C) instruments. Chemical shifts for ^{1}H and ^{13}C are referenced to internal solvent resonances and are reported relative to tetramethylsilane. ^{19}F NMR shifts are referenced to external $CFCl_3$. Neat methanol or ethylene glycol were used as temperature standards in all variable temperature NMR experiments. NMR experiments on air-sensitive samples were conducted in either Teflon valve-sealed tubes (J. Young) or in screw-capped tubes fitted with septa (Wilmad). Circular dichroism (CD) spectra were recorded on a Jasco J-500 spectrophotometer equipped with a JASCO DP-500/AT software package (version 1.2). Air-sensitive samples were prepared in 10 mm path length cylindrical quartz cuvettes (Helma Cells) fitted with Teflon needle valves. Solvent blanks were recorded under identical conditions and the base line subtracted from the experimental spectrum. Molar ellipticities [θ] are reported relative to absorption maxima in units of deg·cm^2·decimol^{-1}. Elemental analyses were performed by Oneida Research Services, Inc., Whitesboro, NY.

Synthesis of K_2Me_2SiCp''[(+)-neomenthylCp](DME)$_2$ (1c). A 250 mL flask with a Teflon inlet valve was charged with Na[(+)-neomenthylCp][11] (10.0 g, 44.2 mmol) in the glovebox. The flask was removed from the glovebox, and under inert atmosphere, THF (150 mL) was added via syringe to the reaction flask. The mixture was stirred, completely dissolving the solids and affording a clear, pale yellow solution. Under an argon flush, a solution of $Me_2Si(Cp''H)Cl$[11a] (9.67 g, 45.0 mmol) in THF (40 mL) was syringed into the stirred solution of the sodium salt. Immediate precipitation of a flocculent, colorless solid (NaCl) occurred. The suspension was stirred at ambient temperature for 10 h. The solvent was then removed *in vacuo*, and pentane (150 mL) was added to the reaction flask. The resulting mixture was filtered, and the colorless precipitate was washed once with pentane (30 mL). The solvent was next removed *in vacuo*, and DME (60 mL) was transferred *in vacuo* onto the residue at −78 °C. This solution was warmed to room temperature and decanted into a sidearm flask containing KH (4.0 g, 0.1 mol) and slowly heated until

(8) (a) Röll, W.; Brintzinger, H. H.; Rieger, B.; Zolk, R. *Angew. Chem., Int. Ed. Engl.* **1990**, *29*, 279−280. (b) Erker, G.; Temme, B. *J. Am. Chem. Soc.* **1992**, *114*, 4004−4006. (c) Gauthier, W.; Corrigan, J. F.; Taylor, N. J.; Collins, S. *Macromolecules*, **1995**, *28*, 3771−3778.

(9) (a) Wiesenfeldt, H.; Reinmuth, A.; Barsties, E.; Evertz, K.; Brintzinger, H. H. *J. Organomet. Chem.* **1989**, *369*, 359−370. (b) Collins, S.; Hong, Y.; Taylor, N. J. *Organometallics* **1990**, *9*, 2695−2703. (c) Collins, S.; Gauthier, W. J.; Holden, D. A.; Kuntz, B. A.; Taylor, N. J.; Ward, D. G. *Organometallics* **1991**, *10*, 2061−2068. (d) Collins, S.; Hong, Y.; Ramachandran, R.; Taylor, N. J. *Organometallics* **1991**, *10*, 2349−2356. (e) Rheingold, A. L.; Robinson, N. P.; Whelan, J.; Bosnich, B. *Organometallics* **1992**, *11*, 1869−1876.

(10) (a) Wild, F. R. W. P.; Zsolnai, L.; Huttner, G.; Brintzinger, H. H. *J. Organomet. Chem.* **1982**, *232*, 233−247. (b) Schäfer, A.; Karl, E.; Zsolnai, L.; Huttner, G.; Brintzinger, H. H. *J. Organomet. Chem.* **1987**, *328*, 87−99.

(11) (a) Giardello, M. A.; Conticello, V. P.; Brard, L.; Sabat, M.; Rheingold, A. L.; Stern, C. L.; Marks, T. J. *J. Am. Chem. Soc.* **1994**, *116*, 10212−10240. (b) Giardello, M. A.; Conticello, V. P.; Brard, L.; Gagné, M. R.; Marks, T. J. *J. Am. Chem. Soc.* **1994**, *116*, 10241−10254. (c) Giardello, M. A.; Yamamoto, Y.; Brard, L.; Marks, T. J. *J. Am. Chem. Soc.* **1995**, *117*, 3276−3277. (d) Fu, P.-F.; Li, Y.; Brard, L.; Marks, T. J. *J. Am. Chem. Soc.* **1995**, *117*, 7157−7168.

(12) Communicated in part: (a) Giardello, M. A.; Eisen, M. S.; Stern, C.; Marks, T. J. *Abstracts of Papers*; 203rd National Meeting of the American Chemical Society, San Fransisco, CA, April 5−10; American Chemical Society: Washington, DC, 1992; INOR 382. (b) Giardello, M. A.; Eisen, M. S.; Stern, C. L.; Marks, T. J. *J. Am. Chem. Soc.* **1993**, *115*, 3326−3327.

gas evolution was evident (45−50 °C). The mixture was then heated to 60 °C until gas evolution had ceased (1−2 h). The mixture was next cooled to ambient temperature, filtered to remove excess KH, concentrated *in vacuo*, and crystallization was induced by scratching the sides of the flask with the magnetic stirbar manipulated by an external magnet. After crystallization, the excess solvent was removed by decantation, and the residual solids were dried *in vacuo* for 3 h yielding $K_2Me_2SiCp''[(+)$-neomenthylCp$](DME)_2$ (27.4 g, 97%) as a highly air- and moisture-sensitive microcrystalline solid. The ligand may be additionally recrystallized from cold (−20 °C) DME: ^{1}H NMR (THF-d_8) δ 5.78 (t, 1H), 5.69 (t, 1H), 5.67 (t, 1H), 3.43 (s, 4H), 3.27 (s, 6H), 3.1 (br m, 1H), 2.16 (s, 6H), 1.84 (s, 6H), 0.85 (d, 3H), 0.80 (d, 3H), 0.75 (d, 3H), 0.57 (s, 3H), 0.55 (s, 3H).

Synthesis of (*R*)-Me$_2$SiCp''[(−)-menthylCp]ZrCl$_2$, (*R*)-2a. $Li_2Me_2SiCp''[(-)$-menthylCp] (5.00g, 12.7 mmol) was dissolved in THF (100 mL). In a separate flask, THF (100 mL) was condensed *in vacuo* at −78 °C onto $ZrCl_4$ (2.96g, 12.7 mmol), and the mixture was warmed to room temperature. These two solutions were simultaneously added in small portions to a well stirred flask containing THF (200 mL) over the course of 6−8 h. Once the addition was complete, the resulting pale yellow solution was heated to reflux for 30 min. The volatiles were then removed *in vacuo*, and the residue was vacuum dried for 3 h. Et_2O (200 mL) was next condensed onto the residue *in vacuo*, and the solution was warmed to ambient temperature. With the aid of an external magnet, the residue was thoroughly mixed, and the solvent was removed *in vacuo*. This procedure was repeated once with Et_2O and twice with pentane. After the second stirring with pentane, the solution was filtered, and the LiCl was washed thoroughly with pentane (3 × 50 mL). The combined extracts were concentrated *in vacuo* and cooled to −78 °C. The resulting pale yellow precipitate was isolated by cold filtration (1.9 g, 29%). An additional 2.5 g (38%) of the zirconocene was recovered from the filtrate by concentrating and slow cooling the saturated pentane solution: total yield, 67% of nearly diastereomerically pure (~8:1 *R:S*) material. The complex was recrystallized to diastereomeric and analytic purity from Et_2O: ^{1}H NMR (benzene-d_6) δ 6.78 (t, 1H), 5.55 (t, 1H), 5.38 (t, 1H), 3.19 (t of d, 1H), 2.52 (m, 1H), 2.19 (m, 1H), 2.05 (s, 3H), 2.04 (s, 3H), 1.82 (s, 3H), 1.79 (s, 3H), 1.71 (m, 2H), 1.50 (br m, 2H), 1.05 (d, 3H), 1.01 (d, 3H), 0.95 (d, 3H), 0.85 (m, 1H), 0.45 (s, 6H); ^{13}C NMR (benzene-d_6) δ 147.9, 135.9, 134.9, 127.2, 126.0, 124.7, 113.4, 111.5, 105.5, 96.8, 47.8, 44.8, 40.8, 35.3, 33.0, 27.3, 25.2, 22.9, 22.2, 17.0, 15.2, 15.0, 12.4, 12.3, −0.5, −0.7; CD (pentane), λ_{max} ([θ]) 372 (−7089), 308 (−14, 515), 274 (+10, 886) nm. Anal. Calcd for $C_{26}H_{40}Cl_2SiZr$: C, 57.53; H, 7.43. Found: C, 57.84; H, 7.58.

Synthesis of (*R*)-Me$_2$SiCp''[(−)-menthylCp]HfCl$_2$, (*R*)-2b. This complex was prepared from $HfCl_4$ (2.44 g, 7.62 mmol) and $Li_2Me_2SiCp''[(-)$-menthylCp] (3.00 g, 7.62 mmol) using the same procedure as for (*R*)-**2a** above: total yield, 3.5 g, 73% of a colorless microcrystalline solid. The complex was recrystallized to diastereomeric and analytic purity from ether/pentane: ^{1}H NMR (benzene-d_6) δ 6.69 (t, 1H), 5.52 (t, 1H), 5.36 (t, 1H), 3.40 (t of d, 1H), 2.42 (m, 1H), 2.17 (m, 1H), 2.05 (s, 3H), 2.04 (s, 3H), 1.88 (s, 3H), 1.81 (s, 3H), 1.71 (m, 1H), 1.48 (br m, 1H), 1.10−1.22 (m, 1H), 0.98 (d, 3H), 0.96 (d, 3H), 0.91 (d, 3H), 0.80 (m, 1H), 0.43 (s, 3H), 0.41 (s, 3H): ^{13}C NMR (benzene-d_6) δ 147.5, 135.1, 133.6, 127.1, 126.2, 124.3, 113,1, 112.2, 105.1, 97.1, 47.7, 44.6, 41.2, 35.6, 33.2, 28.1, 25.5, 23.3, 21.9, 16.8, 15.4, 15.1, 12.2, 13.0, −0.4, −0.6; CD (pentane), λ_{max} ([θ]) 346 (−10,625), 284 (−23,002), 253 (+13,420) nm. Anal. Calcd for $C_{26}H_{40}Cl_2SiHf$: C, 49.09; H, 7.29. Found: C, 49.38; H, 7.41.

Synthesis of (*R/S*)-Me$_2$SiCp''[(+)-neomenthylCp]ZrCl$_2$, (*R,S*)-2c. Method A. This complex was prepared from $ZrCl_4$ (2.96 g, 12.7 mmol) and $Li_2Me_2SiCp''[(+)$-neomenthylCp] (5.00 g, 12.7 mmol) using the same procedure as for (*R*)-**2a** above: total yield, 62% of a pale yellow microcrystalline solid (60/40 *R/S*). The compound was recrystallized from ether/pentane to give a 1:1 *R/S* mixture of diastereomers. **Method B.** This complex was also prepared from $ZrCl_4$ (2.96 g, 12.7 mmol) and $K_2Me_2SiCp''[(+)$-neomenthylCp] (g, 12.7 mmol) using the same procedure as for (*R*)-**2a**: total yield, 56% of a pale yellow microcrystalline solid (60/40 *R/S*). The compound was recrystallized from ether/pentane to give a 1:1 *R/S* mixture: ^{1}H NMR (chloroform-*d*) δ 6.99 (t, 1H), 6.81 (t, 1H), 5.65 (t, 1H), 5.64 (t, 1H), 5.42 (t, 1H), 5.38 (t, 1H), 3.61 (m, 1H), 3.29 (m, 1H), 2.09 (s, 3H), 2.08 (s, 3H), 2.04 (s, 3H), 2.03 (s, 3H), 1.99 (s, 3H), 1.95 (s, 3H), 1.89 (s, 3H), 1.40−1.10 (m, 3H), 1.04 (d, 3H), 0.90 (d, 3H), 0.88 (d, 3H), 0.86 (d, 3H), 0.85 (d, 3H), 0.84 (s, 3H), 0.83 (s, 3H), 0.81 (d, 3H). Anal. Calcd for $C_{26}H_{40}Cl_2SiZr$: C, 57.53; H, 7.43. Found: C, 57.23; H, 7.17.

Synthesis of (*R*)-Me$_2$SiCp''[(−)-menthylCp]ZrMe$_2$, (*R*)-3a. A 100 mL flask was charged with (*R*)-$Me_2SiCp''[(-)$-menthylCp$]ZrCl_2$, (*R*)-**2a**, (1.31 g, 2.42 mmol) and MeLi·LiBr·2(Et_2O) (1.25 g, 4.87 mmol). Toluene (75 mL) was then condensed onto the solids *in vacuo* at −78 °C, and the mixture was warmed to ambient temperature. The resulting solution was then stirred for 24 h at room temperature. The solvent was next removed *in vacuo*, and the residue vacuum was dried for 2 h. Pentane was then condensed onto the residue *in vacuo* at −78 °C, and the mixture was warmed to ambient temperature. The solvent was removed, and the procedure was repeated twice to remove any entrained toluene. The solution was then filtered to remove LiCl and the solids washed with pentane (3 × 25 mL). The combined extracts were concentrated *in vacuo*, and the solution was slowly cooled to −78 °C to yield the diastereomerically pure dimethyl complex (715 mg, 60%). An additional 350 mg (29%) was recovered from the filtrate by concentration and slow cooling to −78 °C: total yield 1.07 g (89%) of colorless crystals; ^{1}H NMR (benzene-d_6) δ 6.71 (t, 1H), 5.51 (t, 1H), 5.32 (t, 1H), 2.78 (t of d, 1H), 2.29 (m, 1H), 1.98 (s, 3H), 1.93 (s, 3H), 1.75 (s, 3H), 1.73 (s, 3H), 1.47 (br m, 2H), 1.25−1.08 (m, 3H), 0.96−0.88 (3d, 6H), 0.44 (s, 3H), 0.37 (s, 3H), −0.18 (s, 3H), −0.27 (s, 3H); ^{13}C NMR (benzene-d_6) δ 140.5, 127.3, 126.2, 124.2, 121.0, 118.8, 113.2, 109.4, 99.2, 91.9, 50.1, 42.6, 41.1, 35.9, 35.7, 33.3, 32.5, 27.4, 25.3, 23.0, 22.0, 16.4, 14.8, 14.4, 11.6, 11.6, 0.4, −0.8. CD (pentane), λ_{max} ([θ]) 351 (+1857), 288 (−10, 036) nm. Anal. Calcd for $C_{28}H_{46}SiZr$: C, 67.00; H, 9.24. Found: C, 67.08; H, 9.21.

Synthesis of (*R*)-Me$_2$SiCp''[(−)-menthylCp]HfMe$_2$, (*R*)-3b. This compound was prepared from (*R*)-$Me_2SiCp''[(-)$-menthylCp$]HfCl_2$, (*R*)-**2b**, (1.40 g, 2.38 mmol) and MeLi (7.0 mL, 9.8 mmol, 1.4 M in Et_2O) using the procedure described for (*R*)-$Me_2SiCp''[(-)$-menthylCp]-$ZrMe_2$ (*R*)-**3a** above: ^{1}H NMR (benzene-d_6) δ 6.60 (t, 1H), 5.48 (t, 1H), 5.33 (t, 1H), 2.75 (br t, 1H), 2.25 (m, 1H), 1.99 (s, 3H), 1.92 (s, 3H), 1.81 (s, 3H), 1.78 (s, 3H), 1.47 (br m, 1H), 1.13 (m, 2H), 0.95 (d, 3H), 0.92 (d, 3H), 0.88 (d, 3H), 0.46 (s, 3H), 0.38 (s, 3H), −0.34 (s, 3H), −0.44 (s, 3H); ^{13}C NMR (benzene-d_6) δ 140.0, 127.3, 124.9, 123.4, 119.0, 117.9, 112.8, 107.9, 101.2, 93.8, 50.4, 42.2, 42.1, 38.7, 35.8, 33.4, 27.6, 25.4, 23.2, 22.1, 16.4, 14.8, 14.4, 11.7, 11.6, 0.7, −0.7. Anal. Calcd for $C_{28}H_{46}SiHf$: C, 57.07; H, 7.87. Found: C, 57.13; H, 7.96.

Synthesis of (*R/S*)-Me$_2$SiCp''[(+)-neomenthylCp]ZrMe$_2$, (*R,S*)-3c. This complex was prepared from (*R/S*)-$Me_2SiCp''[(+)$-neomenthylCp$]ZrCl_2$ (*R,S*)-**2c** (1.6 g, 2.95 mmol) and MeLi (7.2 mL, 10.03 mmol, 1.4 M in Et_2O) using the same procedure as for **3b** above with a (55/45) mixture of diastereomers being isolated: total yield, 87%. Recrystallization from pentane affords a colorless microcrystalline solid (1:1 *R/S*): ^{1}H NMR (toluene-d_8) δ 6.91 (t, 1 H), 6.78 (t, 1H), 5.45 (t, 1H), 5.39 (t, 1H), 5.37 (t, 1H), 5.24 (t, 1H), 3.55−3.45 (br m, 2H), 1.98 (s, 3H), 1.95 (s, 9H), 1.91 (s, 3H), 1.70 (s, 3H), 1.69 (s, 3H), 1.68 (s, 6H), 1.40−1.19 (m, 3H), 1.10 (d, 3H), 1.02 (d, 3H), 0.98 (d, 3H), 0.93 (d, 3H), 0.90 (d, 3H), 0.73 (d, 3H), 0.42 (s, 3H), 0.40 (s, 6H), 0.37 (s, 3H), −0.33 (s, 3H), −0.35 (s, 3H), −0.38 (s, 3H), −0.40 (s, 3H). Anal. Calcd for $C_{28}H_{46}SiZr$: C, 67.00; H, 9.24. Found: C, 67.00; H, 9.29.

Reaction of (*R*)-Me$_2$SiCp''[(−)-menthylCp]ZrMe$_2$ with B(C$_6$F$_5$)$_3$. In the glovebox, a J-Young NMR tube was charged with (*R*)-$Me_2SiCp''[(-)$-menthylCp$]ZrMe_2$, (*R*)-**3a**, (10 mg) and $B(C_6F_5)_3$ (11 mg). The NMR tube was removed from the glovebox, attached to a vacuum line, toluene-d_8 (0.4−0.6 mL) was transferred on the solids *in vacuo*, and the J-Young NMR tube was sealed. Upon shaking and dissolution of the solids, an immediate color change from pale to bright yellow occurred. The sample was then placed in a precooled (0.0 ± 0.2 °C) NMR probe and equilibrated at that temperature for 20 min. Spectra were then recorded using a 45° pulse width, 2 s aquisition time, and 5 s pulse delay: ^{1}H NMR (toluene-d_8, 0.0 °C) (major resonances) δ 6.17 (s, 1H), 5.44 (s, 1H), 4.87 (s, 1H), 2.51 (t, 1H), 1.59 (s, 3H), 1.45 (s, 3H), 1.38 (s, 3H), 1.15 (s, 3H), 0.89 (d, 3H), 0.81 (d, 3H) 0.80 (d, 3H), 0.43 (br s, 3H), 0.23 (s, 3H), 0.22 (s, 3H), 0.12 (s, 3H); (minor resonances) δ 6.24 (s, 3H), 5.42 (s, 3H), 5.18 (s, 3H), 1.89 (t, 1H), 1.72 (s, 3H), 1.70 (s, 3H), 1.50 (s, 3H), 1.37 (s, 3H), 0.95 (d, 3H), 0.78 (d, 3H), 0.70 (d, 3H), 0.36 (s, 3H), 0.30 (s, 3H), 0.19 (br s, 3H), −0.21 (s, 3H); ^{19}F NMR (toluene-d_8, −10.0 °C) (major resonances) δ

−129.5 (d, J_{F-F} = 25.6 Hz, 6F), −155.3 (t, J_{F-F} = 20.7 Hz, 3F), −160.1 (t, J_{F-F} = 19.2 Hz, 6F); (minor resonances) δ −128.7 (d, J_{F-F} = 22.2 Hz, 6F), ~ −155.3 (3F), −160.4 (t, J_{F-F} = 19.2 Hz, 6F).

Reaction of (*R*)-Me$_2$SiCp″[(−)-menthylCp]HfMe$_2$ with B(C$_6$F$_5$)$_3$. In the glovebox, a J-Young NMR tube was charged with (*R*)-Me$_2$SiCp″-[(−)-menthylCp]HfMe$_2$, (*R*)-**3b**, (11 mg) and B(C$_6$F$_5$)$_3$ (11 mg). The NMR tube was removed from the glovebox, attached to a vacuum line, toluene-d_8 (0.4−0.6 mL) was transferred onto the solids *in vacuo*, and the J-Young NMR tube was sealed. Upon shaking and dissolution of the solids, an immediate color change from colorless to pale yellow occurred. NMR spectra were recorded as above: ^{1}H NMR (toluene-d_8, 5.0 °C) (major resonances) δ 6.01 (s, 1H), 5.50 (s, 1H), 4.85 (s, 1H), 2.55 (t, 1H), 1.61 (s, 3H), 1.60 (s, 3H), 1.45 (s, 3H), 1.32 (s, 3H), 0.88 (d, 3H), 0.81 (d, 3H) 0.75 (d, 3H), 0.45 (br s, 3H), 0.31 (s, 3H), 0.20 (s, 3H), 0.18 (s, 3H); (minor resonances) δ 6.21 (s, 3H), 5.65 (s, 3H), 5.19 (s, 3H), 1.88 (s, 3H), 1.80 (s, 3H), 1.48 (s, 3H), 0.28 (s, 3H), 0.15 (s, 3H), −0.12 (s, 3H); ^{19}F NMR (toluene-d_8, −10 °C) (major resonances) δ −132.2 (d, J_{F-F} = 21.8 Hz, 6F), −157.7 (t, J_{F-F} = 20.7 Hz, 3F), −162.6 (t, J_{F-F} = 18.4 Hz, 6F); (minor resonances) δ −131.1 (d, J_{F-F} = 21.4 Hz, 6F), ~ −157.7 (3F), −162.8 (t, J_{F-F} = 18.0 Hz, 6F).

Equilibration of Me$_2$SiCp″[(−)-menthylCp]MMe$^+$MeB(C$_6$F$_5$)$_3^-$ Ion Pairs. In the glovebox, a J-Young NMR tube was charged with (*R*)-Me$_2$SiCp″[R*Cp]MMe$_2$, ((*R*)-**3a** or (*R*)-**3b**; 10−12 mg) and B(C$_6$F$_5$)$_3$ (11 mg). The NMR tube was removed from the glovebox, attached to a vacuum line, toluene-d_8 (0.4−0.6 mL) was transferred onto the solids *in vacuo*, the J-Young NMR tube was then sealed, and the solids were dissolved by shaking. The sample was then placed in a precooled (0.0 ± 0.2 °C) NMR probe and equilibrated at that temperature for 30 min. Spectra were then recorded at various temperatures (−40 to 10 ± 0.2 °C) using a 45° pulse width, 2 s aquisition time, and 10 s pulse delay. The temperature dependence of the cyclopentadienyl protons was monitored, and the relative concentrations of the two ion pairs observed were assayed by integration. The data were fit by least-squares analysis to eq 1. A plot of ln(*K*) (where K = [ion pair]$_a$/[ion pair]$_b$) vs $1/T$ afforded ΔH and ΔS for the equilibrium from the slope and *y*-intercept, respectively.

$$\ln(K) = -\frac{\Delta H}{R}\left(\frac{1}{T}\right) + \frac{\Delta S}{R} \qquad (1)$$

Olefin Polymerization Experiments (above −40°C). Method A. In the glovebox, a 100 mL flamed reaction flask equipped with a magnetic stirring bar was charged with metallocene (5−20 mg) and co-catalyst, and the flask was then reattached to the high vacuum line. A measured amount of toluene was next condensed onto the solids, and the mixture was warmed to 0 °C with stirring for 15 min to preactivate the catalyst. The pale yellow to red solution was then equilibrated at the desired reaction temperature using an external constant temperature bath. Gaseous propylene was next introduced with rapid stirring, and the pressure was maintained at 1 atm by means of a mercury bubbler. After a measured time interval, the reaction was quenched by the addition of acidified methanol. The solvent was removed *in vacuo*, pentane (50 mL) was added, and the mixture was stirred. The polymer was collected by filtration and washed liberally with pentane followed by methanol. The polymer was then dried *in vacuo* for several hours. All volatiles were removed from the filtrate, and the remaining organics were chromatographed on silica with HPLC grade pentane. **Method B.** In the glovebox, 6 mL sample vials equipped with septum caps were charged with metallocene (5−20 mg) and co-catalyst. Toluene (48 mL) was syringed into a flamed 100 mL reaction flask equipped with a large stir bar and a septum-covered sidearm. The reaction flask was reattached to the high vacuum line, and the solvent freeze−pump−thaw was degassed, saturated with 1 atm ethylene or propylene, and equilibrated at the desired temperature using an external constant temperature bath. A measured amount of toluene was then syringed into the vials (removed from the glovebox immediately prior to these experiments) containing the metallocene/co-cocatalyst mixture with a dry, Ar-purged gas-tight syringe. The solution was mixed until all of the solids had dissolved with a characteristic color change. A measured amount of the catalyst solution (2 mL) was then syringed into the reaction flask through the septum via a dry, Ar-purged gas-tight syringe. After a measured time interval with rapid stirring, the polymerization was quenched and worked-up as in method A.

Propylene Polymerization Experiments (Below −40 °C). In the glovebox, a flamed 100 mL reaction flask was charged with metallocene (5−20 mg) and co-catalyst, and the flask was reattached to the high vacuum line. A measured amount of toluene was then condensed onto the solids, and the mixture was warmed to 0 °C with stirring for 15 min to preactivate the catalyst. A measured amount of propylene (3−10 mL) was quickly transferred into the reaction flask *in vacuo* at −78 °C, and the reaction mixture then stirred at the desired temperature. After a measured time interval, the polymerization was quenched and worked-up in an identical manner to the previous polymerization *(vide supra)*.

^{1}H and ^{13}C NMR Assay of Polymer Microstructure. For ^{13}C NMR assays, 100−300 mg of polymer sample was added to a 5 or 10 mm NMR tube followed by 0.7 to 2.5 mL of a 1/6 v/v solution of DMSO-d_6 and 1,2,4-trichlorobenzene, respectively. The sample was preheated with a heat gun until all of the polymer dissolved (130−150 °C). The sample was immediately transferred to the NMR spectrometer with the probehead preequilibrated at 130 ± 1.0 °C. The sample was equilibrated at that temperature for 20 min at which time both spinning and nonspinning shims were adjusted. A 45° pulse width and 2.5 s acquisition time were used with a pulse delay of 5 s. ^{1}H NMR samples were prepared in a similar manner except 1,2-dideutereotetrachloroethane was used as a solvent with 30−100 mg of polymer sample. For the pentane-soluble samples, the solvents C$_6$D$_6$ or CDCl$_3$ were used to measure the ^{1}H and ^{13}C spectra.

Determination of Polymer Molecular Weights. M_n and M_w were determined by GPC analysis at AKZO Research Laboratories on a Waters 150 °C GPC. The polymer solutions were prepared by dissolving each sample in hot (T = 130 °C) 1,2,4-trichlorobenzene and filtered hot through a 0.45 μm filter and analyzed on a bank of 4 μ Styragel HT columns (10^3, 10^4, 10^5, and 10^6). The M_n and M_w values, and the MWD plots were calculated using conventional calibration techniques with polystyrene standards. For the lower molecular weight samples, M_n and M_w/M_n were determined via NMR end-group analysis, GLC, and GC-MS. All measurements were in good agreement (±10−20 %).

X-ray Crystallographic Study of (*R*)-Me$_2$SiCp″[(−)-menthylCp]-ZrR$_2$, ((*R*)-2a,3a). Colorless crystals of **2a** were grown by slow diffusion of pentane into a saturated Et$_2$O solution at −10 °C, while colorless crystals of **3a** were grown by slow cooling of a saturated pentane solution to −30 °C. In each case, the solvent was decanted and Paratone-N (Exxon, dried and degassed at 120 °C/10^{-6} Torr for 24 h) was poured over the crystals in the glovebox. Crystals of **2a** and **3a** of dimensions 0.10 × 0.40 × 0.50 mm and 0.35 × 0.24 × 0.08 mm, respectively, were mounted on glass fibers and transferred to the cold steam (−120 °C) of the Enraf-Nonius CAD4 diffractometer. Unit cell and data collection parameters are summarized in Table 1. Subsequent computations were carried out on a microVax 3600 computer.

Lattice parameters were determined from 25 angle reflections set in the range 18.40° < 2θ < 21.4° and 20.0° < 2θ < 30.8° for **2a** and **3a**, respectively. Systematic absences and successful refinement of the proposed structures showed **2a** and **3a** to crystallize in the orthorhombic and monoclinic space groups $P2_12_12_1$ (no. 19)[16] and $P2_1$ (no. 4),[17] respectively. Intensities of three standard reflections were measured every 1.5 h of X-ray exposure and showed no significant variations. Intensity data were corrected for Lorentz, polarization, and anomalous dispersion effects.[18] Analytical absorption corrections were applied which resulted in transmission factors ranging from 0.75 and 0.94 for

(13) (a) Moeseler, R.; Horvath, B.; Lindenau, D.; Horvath, E. G.; Krauss, H. L. *Z. Naturforsch., B* **1976**, *31B*, 892−893. (b) McIlwrick, C. R.; Phillips, C. S. G.; *J. Chem. Phys. E* **1973**, *6*, 1208−1210. (c) He, M.-Y.; Xiong, G.; Toscano, P. J.; Burwell, R. L., Jr.; Marks, T. J. *J. Am. Chem. Soc.* **1985**, *107*, 641−652.

(14) (a) Massey, A. G.; Park, A. J. *J. Organomet. Chem.* **1964**, *2*, 245−250. (b) Massey, A. G.; Park, A. J. *J. Organomet. Chem.* **1966**, *5*, 218−225.

(15) Prepared by metathesis with LiB(C$_6$F$_5$)$_4$.[14a]

(16) Cromer, D. T.; Waber, J. T. *International Tables for X-ray Crystallography*; The Kynoch Press: Birmingham, England, 1974; Vol. IV, pp 196−197.

(17) Reference 15, Vol. IV, pp 112−113.

(18) Reference 15, Vol. IV, pp 149.

Table 1. Crystallographic Details for (*R*)-Me_2SiCp''[(−)-menthylCp]ZrX_2 ((*R*)-**2,3a**) Complexes

complex	(*R*)-**2a**	(*R*)-**3a**
formula	$ZrCl_2SiC_{26}H_{40}$	$ZrSiC_{28}H_{46}$
formula weight	542.81	501.98
crystal color, habit	colorless, platey	
crystal dimensions (mm)	0.10 × 0.40 × 0.50	0.35 × 0.24 × 0.08
crystal system	orthorhombic	monoclinic
a, Å	9.404(2)	9.501(3)
b, Å	9.817(3)	9.394(3)
c, Å	28.684(7)	15.565(3)
β	90	103.76(2)
V, Å^3	2648(2)	1349(1)
space group	$P2_12_12_1$	$P2_1$
Z	4	2
d(calc), g/cm^3	1.361	1.235
diffractometer	Enraf-Nonius, CAD4	
temperature	−120 °C	
transmission factors range	−0.75−0.94 (numerical)	0.86−0.94 (numerical)
radiation	graphite monochromator; Kα, $\lambda = 0.71069$	
scan type	ω-θ	
2θ range (deg)	2.0−46.0 ($-h+k+l$)	2.0−54.0 ($\pm h+k-l$)
intensities (unique, R_i)	3970 (3302, 0.054)	2096 (2014, 0.033)
intensities > 3σ(I)	2025	1528
no. of parameters	271	270
R	0.056	0.037
R_w for $w = 1/s^2(F_o)$	0.061	0.039
max density in final diff. Fourier map, e/Å^3	0.90	0.59

2a and 0.86 and 0.94 for **3a**. The structures were solved by direct methods,[19] and the non-hydrogen atoms were refined anisotropically. The final cycles of full-matrix least-squares refinement[20] were based on 2025 and 1528 observed reflections ($I > 3.00\sigma(I)$) and 271 and 270 variable parameters for **2a** and **3a**, respectively. The enantiomer was tested, and refinement converged (largest parameter shifts were 0.01 and 0.03 times the esd) with unweighted and weighted agreement factors of $R(F) = 0.056$, $R_w(F) = 0.061$ and $R(F) = 0.037$, $R_w(F) = 0.039$, for **2a** and **3a**, respectively. For each complex, the absolute configuration followed from the known configuration of the chiral auxiliary and was shown to be the (*R*) diastereomer. Additionally, the (*R*)-diastereomer refined more satisfactorily than the corresponding (*S*)-diastereomer ($R_w(F) = 0.061$ vs $R_w(F) = 0.064$ for **2a** and $R_w(F) = 0.039$ vs $R_w(F) = 0.043$ for **3a**). The standard deviations of an observation of unit weight[21] for **2a** and **3a** were 2.08 and 1.29, respectively. The weighting schemes were based on counting statistics and included a factor ($p = 0.03$) to downweight the intense reflections. The maximum and minimum peaks in the final difference Fourier maps corresponded to 0.90 and −0.54 (e Å^{-3}) for (*R*)-**2a** and 0.59 and −0.41 (e Å^{-3}) for (*R*)-**3a**, respectively. Neutral atom scattering factors were taken from Cromer and Waber.[22] Anomalous dispersion effects were included in *F*calc;[23] the values for $\Delta f'$ and $\Delta f''$ were those of Cromer.[24] All calculations were performed using the TEXSAN[25] crystallographic software package of Molecular Structure Corporation.

Results

This section begins with a discussion of chiral group 4 metallocene synthesis and characterization. Aspects of the structures of two representative, diastereomerically pure metallocenes are discussed as well as their absolute configurations. The solution chiroptical properties are then presented, followed by the generation of active polymerization catalysts and the experimental details of the polymerization procedures. Solution structural dynamic processes in borane-derived ion pairs are then analyzed as well as the thermal stability of such species. Catalyst activities and the microstructures of the resulting polyolefins are then presented, including the results from the assays of polymer stereoregularity, molecular weight, and molecular weight distribution.

Synthesis of Chiral Metallocene Dichlorides. Several synthetic routes were examined for the preparation of the group 4 dichlorides $Me_2SiCp''(R^*Cp)MCl_2$ (R* = (−)-menthyl, (+)-neomenthyl; M = Zr, Hf). The highest yield route was via reaction of the corresponding $Li_2Me_2SiCp''(R^*Cp)$ reagents with $MCl_4(THF)_2$ in THF at ambient temperature under high dilution conditions (eq 2). Reaction of $K_2Me_2SiCp''(R^*Cp)$ with $MCl_4(THF)_2$ (M = Zr, Hf) afforded the metallocenes in lower yield and with similar diastereoselectivity in the incipient complexation reaction *(vida infra)*. Extraction with pentane followed by concentration and slow cooling afforded the metallocenes as pale-yellow to colorless microcrystalline solids. Subsequent recrystallization from diethyl ether/pentane led to the analytically pure complexes.

$$\underset{\mathbf{1}}{Li_2Me_2SiCp''[R^*Cp]} + MCl_4(THF)_2 \xrightarrow[2.\ \text{Pentane}]{1.\ \text{THF}} \underset{\mathbf{2}}{Me_2SiCp''(R^*Cp)MCl_2} + 2LiCl \quad (2)$$

R* = (−)-menthyl M = Zr (**2a**)
Hf (**2b**)
R* = (+)-neomenthyl M = Zr (**2c**)

The readily interpretable ^1H and ^{13}C NMR spectra of the diamagnetic, chiral Zr and Hf complexes indicate that initial diastereoselectivity in the formation of these metallocenes has only a slight dependence on the identity of the chiral auxiliary. The two diastereomers have a pseudoenantiomorphous relationship and are related by the diastereoface of the chiral cyclo-

(19) Structure Solution Methods: SHELXS-86: Sheldrick, G. M. SHELXS-86. In *Crystallographic Computing 3*; Sheldich, G. M.; Kruger, C., Goddard, R., Eds.; Oxford University Press: New York, 1985; pp 175−189.

(20) Least-squares: function minimized: $Sw(|F_o| - |F_c|)^2$ where $w = 4F_o^2/s2(F_o^2)$; $s^2(F_o^2) = [S^2(C + R^2B) + (pF_o^2)^2]/Lp^2$; *S* = scan rate; *C* = total integrated peak count; *R* = ratio of scan time to background counting time; *B* = total background count; Lp = Lorentz-polarization factor; *p* = *p*-factor.

(21) Standard deviation of an observation of unit weight: $[Sw(|F_o| - |F_c|)^2/(N_o - N_v)]^{1/2}$ where N_o = number of observations and N_v = number of variables.

(22) Reference 16, Vol. IV, p 149.

(23) Ibers, J. A.; Hamilton, W. C. *Acta Crystallogr.* **1964**, *17*, 781.

(24) Reference 20, Vol. IV, p 149.

(25) TEXSAN, TEXSAN Structure Analysis Package, Molecular Structure Corporation, 1985.

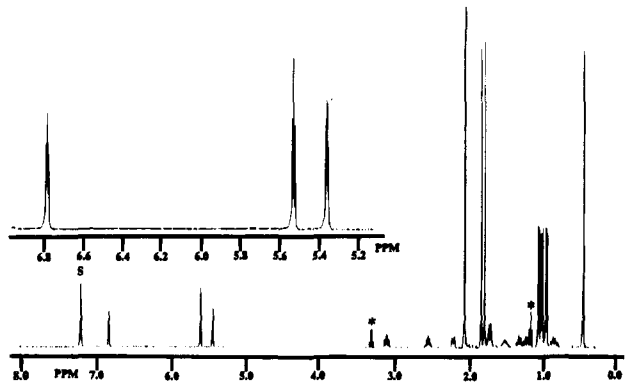

Figure 1. ^{1}H NMR spectrum (400 MHz) of $Me_2SiCp''[(-)$-menthylCp]-$ZrCl_2$ (**2a**) as a solution in benzene-d_6. S denotes residual protons of the deuterated solvent. * denotes residual Et_2O from recrystallization.

pentadienide which is bound to the metal center (**J**(*S*) and **K**(*R*)).[26] The ^{1}H NMR spectra of **2a**–**c** have well-resolved features in the cyclopentadienyl regions which provide a direct assay of diastereomeric purity. Metallocenes bearing the (−)-menthyl auxiliary can be readily isolated as diastereomerically

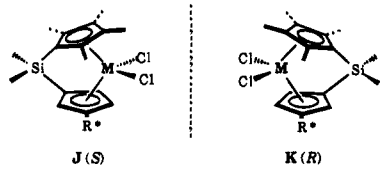

J (*S*) **K** (*R*)

pure complexes after one recrystallization. The Zr and Hf complexes exhibit a single set of resonances in the ^{1}H NMR spectra of the bound ancillary ligand (Figure 1). However, metallocenes bearing the (+)-neomenthyl auxiliary can only be obtained as pseudoracemates with ^{1}H NMR spectra exhibiting two sets of chiral ancillary ligand resonances. The ^{1}H NMR spectrum of a solution prepared from a single crystal of **2c** suggested that *both isomers cocrystallize in the same unit cell in a 1:1 ratio.* Although unusual, this cocrystallization phenomena was also observed in the synthesis of related organolanthanide $CH(TMS)_2$ and $N(TMS)_2$ complexes bearing the same ancillary ligand.[11a]

Unlike organolanthanide $Me_2SiCp''(R*Cp)Ln(\mu\text{-}Cl)_2Li(ether)_2$ complexes,[11a] the present group 4 metallocene dichlorides are configurationally stable in donor solvents at both ambient and elevated temperatures. The irreversibility of the R*Cp coordination precludes selective enrichment of either antipode of the metallocene by Lewis base-induced chemical equilibration.[11a] Thus, the diastereoselectivity of initial complexation limits the yield of optically pure metallocene obtainable after fractional crystallization. However, the yield of optically pure metallocene is still relatively high (>70%) in the case of the (−)-menthyl derivatives. The metallocene dichlorides are thermally stable in hydrocarbon (toluene, benzene) and ether (tetrahydrofuran, diethyl ether) solutions for weeks at 25 °C but decompose over the course of several days in halogenated solvents (chloroform, methylene chloride).

Synthesis of Chiral Metallocene Dimethyls. The reaction between the metallocene dichlorides $Me_2SiCp''(R*Cp)MCl_2$ and excess MeLi in toluene affords $Me_2SiCp''(R*Cp)MMe_2$ complexes in high yield and purity (eq 3). Alkylation proceeds with net retention of configuration at the metal center *(vide infra)*

$$\underset{\mathbf{2}}{Me_2SiCp''(R*Cp)MCl_2} + MeLi \xrightarrow[\text{2. pentane}]{\text{1. toluene}} \underset{\mathbf{3}}{Me_2SiCp''(R*Cp)MMe_2} + 2LiCl \quad (3)$$

R* = (−)-menthyl M = Zr (**3a**)
Hf (**3b**)
R* = (+)-neomenthyl M = Zr (**3c**)

and is independent of the chiral auxiliary, solvent, and reaction temperature. Only trace amounts (<5%) of the other metal-based diastereomer can be detected in the ^{1}H NMR of the initial reaction products. The dimethyl complexes can be extracted with, and crystallized from, pentane to afford the analytically pure metallocenes. Isolation of diastereomerically pure metallocene complexes is only possible for the (−)-menthyl derivatives. Thus, a single recrystallization from pentane provides diastereomerically pure Zr and Hf complexes. As with the dichlorides, the (+)-neomenthyl derivative crystallizes as a 1:1 pseudoracemate with single crystals containing both the *(R)*- and *(S)*- planar chiral configurations of the chiral cyclopentadienyl, thus precluding straightforward isolation of diastereomerically pure **3c**. The readily interpretable ^{1}H NMR spectra of **3a**–**c** exhibit characteristic resonances at relatively high field for the Zr–Me protons (δ −0.18 to −0.40 ppm).[7i,27] The metallocene dimethyl complexes are configurationally and thermally stable in hydrocarbon (toluene, benzene) and ether (THF, diethyl ether) solvents for weeks but decompose over the course of hours in halogenated solvents (chloroform, methylene chloride).

Molecular Structure of $Me_2SiCp''[(-)$menthylCp$]ZrX_2$ Complexes (*(R)*-2,3a). Low temperature single crystal diffraction studies of optically pure **2a** and **3a** reveal a single planar chiral configuration of the diastereotopic, chirally-substituted cyclopentadienyl group, the (*R*)-configuration, in both molecular structures (Figure 2, parts A and B, respectively). Data collection information and important metrical parameters are given in Tables 1 and 2, respectively. The complexes (*R*)-**2a** and (*R*)-**3a** adopt the pseudotetrahedral bent metallocene structure typical of Cp_2MX_2 complexes.[7a,b,27] All non-hydrogen atoms were refined anisotropically. The complexes exhibit Zr–C_{ring} distance dispersions typical of this type of linked cyclopentadienyl ligation. The Zr–C_{ring} distances proximal to the Me_2Si bridge are shorter than the corresponding distal Zr–C_{ring} distances, and the average bond lengths and angles in (*R*)-**2a** and (*R*)-**3a** compare favorably with previously characterized dimethylsilanobridged complexes.[28]

The (−)-menthyl chiral auxiliary in (*R*)-**2a** and (*R*)-**3a** is located on a single side of the asymmetric complex and adopts a similar conformation in both complexes with the bulky *i*-Pr group oriented *anti*[11a] to the Me_2Si bridge. The cyclohexyl group of the chiral auxiliary adopts a chair conformation in which all three substituents occupy equatorial positions. This conformation has been previously observed in structurally

(26) For nomenclature guidelines, see: (a) Sloan, T. E. *Top. Stereochem.* **1981**, *12*, 1–36. (b) Stanley, K.; Baird, M. C. *J. Am. Chem. Soc.* **1975**, *97*, 6598–6599. (c) Krow, G. *Top. Stereochem.* **1970**, *5*, 31–68.

(27) Cardin, D. J.; Lappert, M. F.; Raston, C. L. *Chemistry of Organo-Zirconium and -Hafnium Compounds*; Ellis Horwood, Chichester, 1986; pp 68–180.

(28) (a) Bajgur, C. S.; Tikkanen, W. R.; Petersen, J. L. *Inorg. Chem.* **1985**, *24*, 2539–2546. (b) Wiesenfeldt, H.; Reinmuth, A.; Barsties, K. E.; Brintzinger, H. H. *J. Organomet. Chem.* **1989**, *369*, 359–370. (c) Burger, P.; Hartmann, K.; Diebold, J.; Brintzinger, H. H. *J. Organomet. Chem.* **1991**, *417*, 9–27.

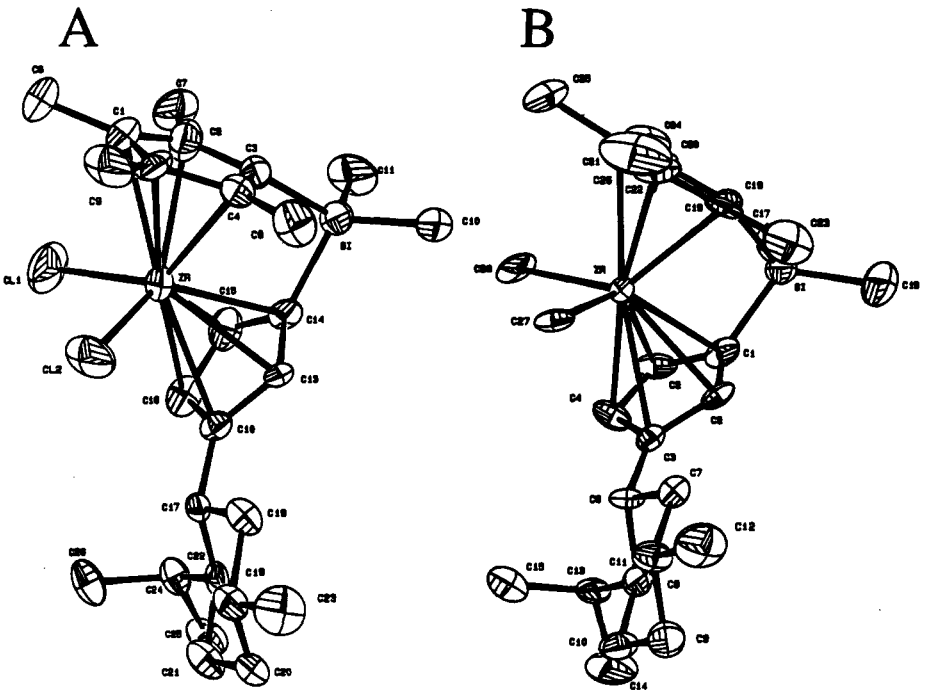

Figure 2. Perspective ORTEP drawing of the molecular structure of (A) (*R*)-Me_2SiCp''[(−)-menthylCp]$ZrCl_2$ ((*R*)-**2a**) and (b) (*R*)-Me_2Si-Cp''[(−)-menthylCp]$ZrMe_2$ ((*R*)-**3a**). All non-hydrogen atoms are represented by thermal ellipsoids drawn to encompass 50% probability.

Table 2. Selected Metrical Parameters for Chiral Organozirconium Complexes

(*R*)-**2a**		(*R*)-**3a**	
Distances (Å)			
Zr−Cl(1)	2.430(4)	Zr−C(28)	2.30(1)
Zr−Cl(2)	2.408(3)	Zr−C(27)	2.265(8)
Zr−C(1)	2.60(1)	Zr−C(21)	2.58(1)
Zr−C(2)	2.50(1)	Zr−C(20)	2.516(9)
Zr−C(3)	2.46(1)	Zr−C(19)	2.468(9)
Zr−C(4)	2.47(1)	Zr−C(18)	2.474(9)
Zr−C(5)	2.57(1)	Zr−C(22)	2.59(1)
Zr−C(12)	2.616(9)	Zr−C(3)	2.642(8)
Zr−C(13)	2.572(8)	Zr−C(2)	2.519(7)
Zr−C(14)	2.466(9)	Zr−C(1)	2.485(8)
Zr−C(15)	2.45(1)	Zr−C(5)	2.476(9)
Zr−C(16)	2.55(1)	Zr−C(4)	2.553(9)
Angles (deg)			
Cl(1)−Zr−Cl(2)	98.6(2)	C(27)−Zr−C(28)	93.8(4)
Cg(1)−Zr−Cg(2)[a]	126.6	Cg(1)−Zr−Cg(2)	127.3
Cp*(1)−Zr−Cp*(2)[b]	118.6	Cp*(1)−Zr−Cp*(2)	120.2
C(10)−Si−C(11)	107.4(6)	C(16)−Si−C(17)	108.0(6)
C(3)−Si−C(14)	93.6(4)	C(19)−Si−C(1)	96.6(4)
Zr−C(4)−C(8)	121.0(7)	Zr−C(18)−C(23)	120.9(6)
Zr−C(5)−C(9)	125.6(7)	Zr−C(22)−C(26)	125.7(8)
Zr−C(1)−C(6)	124.0(9)	Zr−C(21)−C(25)	122.9(8)
Zr−C(2)−C(7)	121.1(9)	Zr−C(20)−C(24)	122.5(8)
Zr−C(12)−C(17)	129.1(6)	Zr−C(3)−C(6)	125.8(5)

[a] Cg = ring centroid. [b] Cp* = Cp mean plane.

characterized (η^5-Cp)(η^5-(−)-menthylCp)$TiCl_2$[29] and (+)-(η^5-(−)-menthylCp)Ru(CO)P-$(C_6H_5)_3Cl$.[30] Unlike the achiral and C_2-symmetric predecessors, the plane formed by the two ring centroids and the metal center in the present complexes *unevenly bisects* the X−Zr−X angle (**L**, $\alpha_1 \neq \alpha_2$). This disparity is greater in (*R*)-**3a** ($\alpha_1 = 42.1°$ and $\alpha_2 = 52.0°$) than it is in (*R*)-**2a** ($\alpha_1 = 46.7°$ and $\alpha_2 = 51.8°$). Additionally, the silicon atom of the dimethylsilano bridge in (*R*)-**3a** is further displaced from this plane (0.577 Å) than in (*R*)-**2a** (0.347 Å). Some of these

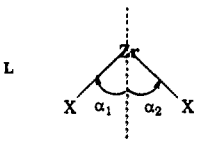

structural distortions likely arise from Zr−X−R* repulsive interactions involving the Zr−X group proximal to the chiral auxiliary. In each of the current structures, the Zr−X group proximal to the chiral auxiliary is bent out of the Cg−Zr−Cg plane by 52°. The increases of the Zr−C(3)−C(6) angle in (*R*)-**3a** from 125.8(5)° to the 129.1(6)° observed for the Zr−C(12)−C(17) angle in (*R*)-**2a** suggests that there are greater Zr−X−R* repulsive interactions for X = Cl. However, there are no exceptionally close nonbonded intermolecular contacts observed in either metallocene. Figure 3 clearly illustrates the coordination asymmetry in (*R*)-**3a**.

Circular Dichroism Spectroscopy of Me_2SiCp''[(−)-menthylCp]MCl_2 Complexes ((*R*)-2a,2b). Circular dichroism (CD) spectra of (*R*)-**2a** and -**2b** were recorded in the 250−450 nm wavelength range as pentane solutions and exhibit three well-resolved absorption maxima. The two lower energy bands (Figure 4) are most likely ligand-to-metal charge transfer (LMCT) transitions,[31] while the highest energy feature is probably a LMCT or $\pi \rightarrow \pi^*$ transition,[32] localized mainly on the π-ancillary ligands. For the pair of isoleptic complexes Me_2-$SiCp''$[(−)-menthylCp]MCl_2 (M = Zr, Hf), the absorption maxima display a significant metal dependence with the Hf complex exhibiting maxima at higher energy (Figure 4). This supports the assignment of the two lower energy bands to LMCT with the more easily reduced[33] Zr complex having absorption maxima at lower energies. However, if the higher energy bands are due to $\pi \rightarrow \pi^*$ transitions exclusively localized on the

(29) Cesarotti, E.; Kagan, H. B.; Goddard, R.; Krüger, C. *J. Organomet. Chem.* **1978**, *162*, 297−309.
(30) Cesarotti, E.; Ciani, G.; Sironi, A. *J. Organomet. Chem.* **1981**, *216*, 87−95.
(31) Harrigan, R. W.; Hammond, G. S.; Gray, H. B. *J. Organomet. Chem.* **1974**, *81*, 79−85.
(32) Wagner, B. O.; Ebel, H. F. *Tetrahedron* **1970**, *26*, 5155.
(33) (a) Lappert, M. F.; Raston, C. L. *J. Chem. Soc., Chem. Commun.* **1981**, 173. (b) Lappert, M. F.; Raston, C. L. *J. Chem. Soc., Dalton Trans.* **1984**, 893.

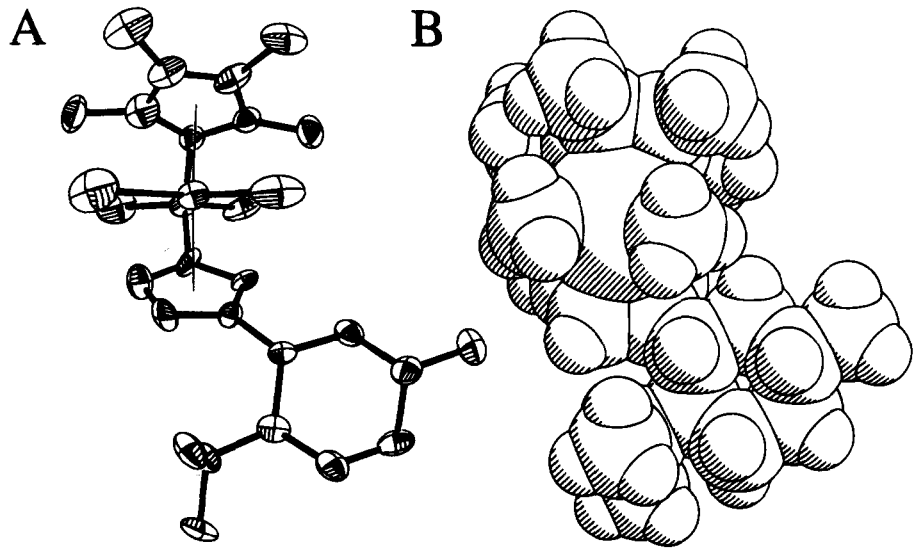

Figure 3. (A) Perspective ORTEP drawing of the molecular structure of (*R*)-Me_2SiCp''[(−)-menthylCp]$ZrMe_2$ ((*R*)-**3a**) viewed along the Cg(1)−Zr−Cg(2) plane. All non-hydrogen atoms are represented by thermal ellipsoids drawn to encompass 50% probability. (B) Perspective space-filling model of the molecular structure of (*R*)-Me_2SiCp''[(−)-menthylCp]$ZrMe_2$ ((*R*)-**3a**) viewed along the Cg(1)−Zr−Cg(2) plane.

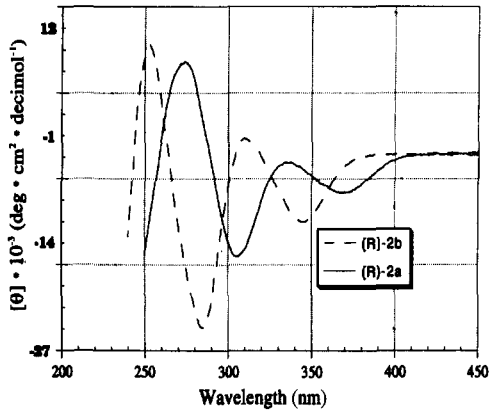

Figure 4. Circular dichroism spectra of (*R*)-Me_2SiCp''[(−)-menthylCp]-$ZrCl_2$ ((*R*)-**2a**) and (*R*)-Me_2SiCp''[(−)-menthylCp]$HfCl_2$ ((*R*)-**2b**) as solutions in pentane in the 250−450 nm wavelength range.

π-ancillary ligands,[32] they should be relatively uneffected by the identity of the isoelectronic metal center, which is not the case.

The CD spectra of the isoleptic pair (*R*)-**2a** and (*R*)-**2b** (Figure 4) have very similar although shifted curve morphologies and display identical Cotton effects. These observations argue for identical configurational assignments. The *(R)*-configuraion of **2a** was unambiguously determined by single crystal diffraction *(vide supra)*. In light of the CD spectra of **2b** and the aforementioned diffraction study of **2a**, the *(R)*-configuration is assigned to the Hf metallocene **2b**. Except for the parent $(R^*Cp)_2MCl_2$ and $(R^*Cp)CpMCl_2$ (R^* = (−)-menthyl or (+)-neomenthyl; M = Ti or Zr) complexes studied by Kagan and co-workers,[34] to our knowledge there are no other reports on the solution chiroptical properties of chiral Zr or Hf metallocenes available for comparison. Recently, Bosnich and co-workers reported[9e] solution chiroptical properties of two related titanocenes but did not report on the Zr derivatives.

Generation of Active Olefin Polymerization Catalysts. The C_1-symmetric metallocene dichloride complexes are converted to catalytically active species by reaction with excess (20−2000 equiv) methylalumoxane in toluene at ambient temperature (eq 4). Presumably the alumoxane alkylates the

$$\underset{\mathbf{2}}{Me_2SiCp''(R^*Cp)MCl_2} + MAO \xrightarrow{\text{toluene}} Me_2SiCp''(R^*Cp)MMe^+MAO^- \quad (4)$$

metallocene to afford the dimethyl species which then undergoes methide abstraction[7g] forming the methyl cation *(vida infra)*. Methylalumoxane is perhaps the best known and most widely studied cocatalyst in homogeneous metallocene Ziegler−Natta catalysis.[1] MAO is an oligomeric organoaluminum reagent formed from the controlled partial hydrolysis of trimethyl aluminum (eq 5). The serendipitous discovery[35] led to extensive investigation of homogeneous α-olefin polymerization catalyst

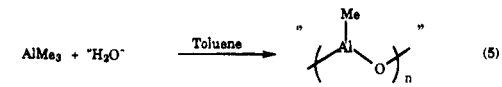

(5)

systems.[1−6] Although the exact structure of MAO is not well-defined, electrodialysis,[36] chemical trapping,[37] model synthetic,[7e,f,38−40] XPS,[41] surface chemical,[42] NMR spectroscopic,[7g] and theoretical studies[5,43] all argue that the role of this and other Lewis acidic co-catalysts is to abstract an alkide/hydride ion

(34) Cesarotti, E.; Kagan, H. B.; Goddard, R.; Kruger, C. *J. Organomet. Chem.* **1978**, *162*, 297−309.

(35) Sinn, H.; Kaminsky, W.; Vollmer, H. J.; Woldt, R. *Angew, Chem., Int. Ed. Engl.* **1980**, *19*, 390.

(36) Dyachkovskii, F. S.; Shilova, A. K.; Shilov, A. Y. *J. Polym. Sci., Part C* **1967**, 2333−2339.

(37) Eisch, J. J.; Piotrowski, A. M.; Brownstein, S. K.; Gabe, E. J.; Lee, F. L. *J. Am. Chem. Soc.* **1985**, *107*, 7219−7220.

(38) (a) Jordan, R. F.; LaPointe, R. F.; Bradley, P. K.; Baenziger, N. *Organometallics* **1989**, *8*, 2892−2903 and references therein. (b) Jordan, R. F.; Echols, S. F. *Inorg. Chem.* **1987**, *26*, 383−386. (c) Jordan, R. F.; LaPointe, R. F.; Bagjur, C. S.; Echols, S. F.; Willett, R. *J. Am. Chem. Soc.* **1987**, *109*, 4111−4113. (d) Shapiro, P. J.; Cotter, W. D.; Schaefer, W. P.; Labinger, J. A.; Bercaw, J. E. *J. Am. Chem. Soc.* **1994**, *116*, 4623−4640.

(39) (a) Bochmann, M.; Jagger, A. J.; Nichols, J. C. *Angew. Chem., Int. Ed. Engl.* **1990**, *29*, 780−782 and references therein. (b) Bochmann, M.; Wilson, L. M. *J. Chem. Soc., Chem Commun.* **1986**, 1610−1611.

(40) (a) Hlatky, G. G.; Turner, H. W.; Eckman, R. R. *J. Am. Chem. Soc.* **1989**, *111*, 2728−2729. (b) Taube, R.; Krukowa, L. *J. Organomet. Chem.* **1988**, *347*, C9−C11.

(41) Gassman, P. G.; Callstrom, M. R. *J. Am. Chem. Soc.* **1987**, *109*, 7875−7876.

(42) Dahmen, K. H.; Hedden, D.; Burwell, R. L., Jr.; Marks, T. J. *Langmuir* **1988**, *4*, 1212−1214.

(43) (a) Jolly, C. A.; Marynick, D. S. *J. Am. Chem. Soc.* **1989**, *111*, 7968−7974. (b) Lauher, J. W.; Hoffman, R. J. *J. Am. Chem. Soc.* **1976**, *93*, 1729−1742.

from the group 4 metal to produce a "cationic", 14 electron metallocene alkyl/hydride. In the present study, MAO was used as a cocatalyst so that direct comparisons of activity, molecular weight, molecular weight distribution, and polymer microstructure could be made with known metallocene/MAO systems.

The C_1-symmetric metallocene dimethyl complexes are converted to catalytically active species by reaction with MAO or a boron cocatalyst in toluene. These cocatalysts produce "cationic" species by either methide abstraction (eqs 6–8) or protonolysis (eq 9).[44,45] $R_3NH^+B(C_6F_5)_4^-$ was used to prepare the first crystallographically characterized base-free "cationic" metallocene $Cp'_2ThMe^+B(C_6F_5)_4^-$.[44b] The choice of amine in eq 9 is critical since *in situ* generation of the "cationic" species incurs the risk of trialkylamine coordination to the product metallocene cation, thus diminishing catalytic activity *(vide infra)*. $B(C_6F_5)_3$ was used to prepare the first crystallography characterized base-free "cationic" zirconocenes,[7d,f] $L_2ZrMe^+MeB(C_6F_5)_3^-$ (L = C_5H_5, 1,2-$Me_2C_5H_3$, Me_5C_5). Significantly, the use of this reagent to generate "cationic" species was the first *direct* observation of the abstractive role of Lewis acids in homogeneous Ziegler–Natta catalyst activation.

$$\underset{\mathbf{3}}{Me_2SiCp''(R^*Cp)MMe_2} + MAO \xrightarrow{\text{toluene}} Me_2SiCp''(R^*Cp)MMe^+MAO^- \quad (6)$$

$$\underset{\mathbf{3}}{Me_2SiCp''(R^*Cp)MMe_2} + B(C_6F_5)_3 \xrightarrow{\text{toluene}} Me_2SiCp''(R^*Cp)MMe^+MeB(C_6F_5)_3^- \quad (7)$$

$$\underset{\mathbf{3}}{Me_2SiCp''(R^*Cp)MMe_2} + Ph_3C^+B(C_6F_5)_4^- \xrightarrow{\text{toluene}} Me_2SiCp''(R^*Cp)MMe^+B(C_6F_5)_4^- + Ph_3CMe \quad (8)$$

$$\underset{\mathbf{3}}{Me_2SiCp''(R^*Cp)MMe_2} + R_3NH^+B(C_6F_5)_4^- \xrightarrow{\text{toluene}} Me_2SiCp''(R^*Cp)MMe^+B(C_6F_5)_4^- + CH_4 + R_3N \quad (9)$$

Use of $Ph_3C^+B(C_6F_5)_4^-$ in generating "cationic" metallocenes (eq 8) was reported by Chien and co-workers.[2d] This reagent has the advantage of introducing weakly coordinating $B(C_6F_5)_4^-$ without coproduction of a potentially coordinating/inhibiting Lewis base ($R_2R'N$).[45]

Without exception, the present C_1-symmetric metallocene methyl cations were not isolable due to thermal lability both in solution and in the solid state. Aged catalyst solutions (24 h to 25 °C) exhibit little or no polymerization activity. The presence of CH_4 in the ^1H NMR of decomposed catalyst solutions implicates C–H activation as at least one of the possible decomposition pathways. Recently, Bergman and co-workers observed intramolecular C–H activation of the (+)-neomenthyl chiral auxilliary in (+)-neomenthylCpMCH$_3$PR$_3^+$ (M = Ir or Rh) complexes to yield CH_4 and an olefin complex.[46] In addition, there have been other decomposition pathways identified for "cationic" metallocenes. Thus, electrophilic "cationic" metallocenes have been shown to abstract F^- from PF_6^- [47] and $Al(CH_3)_2F$.[48] Additionally, the fluoride-bridged complex [(1,2-$Me_2Cp)_2(CH_3)Zr(\mu$-F)Zr(CH_3)(1,2-$Me_2Cp)_2$]$^+CH_3B(C_6F_5)_3^-$ and the C–H activated complex [(1,3-*t*-BuCp)(1-*t*-Bu-3-C$(CH_3)_2$-CH_2Zr]$^+CH_3B(C_6F_5)_3^-$ (**M**) are crystallography characterized decomposition products.[7f] The former may be viewed as an adduct between neutral (1,2-$Me_2Cp)_2Zr(CH_3)F$ and cationic (1,2-$Me_2Cp)_2Zr(CH_3)^+CH_3B(C_6F_5)_3^-$. The neutral fluoride is likely formed via *ortho*-abstraction of fluoride from either (1,2-$Me_2Cp)_2Zr(CH_3)(C_6F_5)$ or (1,2-$Me_2Cp)_2Zr(C_6F_5)^+CH_3B(C_6F_5)_3^-$. Complex **M** is formed by C–H activation of a cyclopentadienyl *t*-Bu substituent with concomitant release of CH_4.[7f]

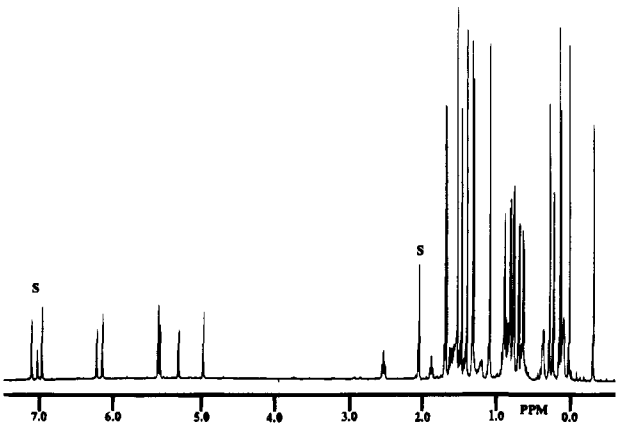

Figure 5. ^1H NMR spectrum (600 MHz) of the reaction product of (*R*)-Me_2SiCp''[(−)-menthylCp]$ZrMe_2$ **3a** with excess $B(C_6F_5)_3$ as a solution in toluene-d_8 at 0 °C. S denotes residual protons of the deuterated solvent.

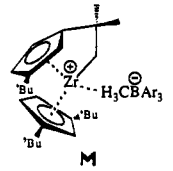

M

The reaction products of eqs 4, 6, 8, and 9 form dark red/brown solutions and upon standing, undergo phase separation from toluene to yield dark oils. This precludes complete characterization of these "cationic" species. However, the metallocene reaction products of eq 7 are thermally stable and soluble in toluene below 5 °C and may be characterized spectroscopically. ^1H NMR spectra of the products of the reaction of $B(C_6F_5)_3$ with diastereomerically pure (*R*)-**3a** (Figure 5) or (*R*)-**3b** indicate the presence, in either case, of *two methyl cations*. Characteristic ^1H resonances[7f] of the Zr^+–Me and B^-–Me groups are apparent with the latter peaks exhibiting the expected ^{10}B, ^{11}B quadrupolar broadening.[49] In the series of compounds $Cp'_2ZrCH_3^+A^-$, (1,2-$Me_2Cp)_2ZrCH_3^+A^-$, and $Cp_2ZrCH_3^+A^-$ (A^- = $CH_3B(C_6F_5)_3^-$) the B–Me resonances are increasingly deshielded at δ −0.30, 0.02, and 0.10 ppm, respectively.[7f] The B–Me resonances of the minor and major products of eq 7 (R* = (−)-menthyl and M = Zr) are further deshielded at δ 0.18 and 0.44 ppm, respectively. There appears to be a qualitative correlation between the degree of coordinative unsaturation of the metallocene and the ^1H chemical shift of the B–Me resonance, i.e., as the metallocene becomes more

(44) (a) Lin, Z.; Le Marechal, J.-F.; Sabat, M.; Marks, T. J. *J. Am. Chem. Soc.* **1987**, 4127–4129. (b) Yang, X.; Stern, C. L.; Marks, T. J. *Organometallics* **1991**, *10*, 840–842. (c) Ewen, J. A.; Elder, M. J. European Patent Application 426,638, 1991.

(45) (a) Turner, H. W.; Hlatky, G. G. PCT Int. Appl. WO 88/05793 (Eur. Pat. Appl. EP 211004, 1988). (b) Ewen, J. A.; Elder, M. J. European Patent Application 427,697, 1991.

(46) Ma, Y.; Bergman, R. G. *Organometallics* **1994**, *13*, 2548–2550.

(47) Jordan, R. F.; Dasher, W. E.; Echols, S. F. *J. Am. Chem. Soc.* **1986**, *108*, 1718.

(48) Zambelli, A.; Longo, P. Grassi, A. *Macromolecules* **1989**, *22*, 2186–2189.

(49) (a) Nöth, H.; Wracker, B. *Nuclear Magnetic Resonance Spectroscopy of Boron Compounds*; Springer Verlage: Berlin, 1978; Chapters 4 and 7. (b) Onak, T. *Organoborane Chemistry*; Academic: New York, 1975; Chapter 2.

coordinatively/sterically unsaturated, the anion becomes more closely associated with the cationic center through $Zr^-—H_3C—B^-$ bridging. This spectroscopic trend is verified in the crystal structures of the related, achiral $Cp'_2ZrCH_3^+A^-$ and $(1,2\text{-}Me_2\text{-}Cp)_2ZrCH_3^+A^-$ ($A^- = CH_3B(C_6F_5)_3^-$) complexes.[7f] The sterically demanding Cp′ ligands in the former elongate the Zr—CH_3B distance to 2.604(7) Å compared to 2.549(3) Å in the latter (both distances are significantly greater than those of the corresponding Zr—CH_3 σ-bonds in the complexes, 2.223(6) and 2.252(4) Å, respectively). This bridging interaction should be viewed as relatively weak and resulting from a balance between coulombic attractions and unfavorable steric repulsions. Nevertheless, the NMR data suggest high levels of coordinative unsaturation for the (*R*)-**3a** and (*R*)-**3b**-derived cations.

Magnetization transfer experiments indicate that the two product isomers in eq 7 are in *slow exchange* on the NMR time scale at 0 °C, and thus homonuclear decoupling experiments can be used to make assignments within each ion pair. ^{19}F NMR reveals the presence of three sets of major and minor resonances. The ratio of the integrals for the major and minor C_6F_5 resonances are equal within experimental error to the ratios of the major and minor isomers derived from the ^1H NMR. The *para* fluorine signals exhibit the usual 15—20 ppm upfield shift upon quaternization of the triarylborane.[7f]

Metallocene Cation—Anion Pairs. Solution Dynamics. In previously characterized (η^5-$1,2\text{-}Me_2C_5H_3)_2ZrMe^+MeB(C_6F_5)_3^-$, it was shown that there are two discernible pathways for the permutation of the diastereotopic methyl groups of the 1,2-Me_2-Cp ligands (eqs 10 and 11).[7e,f] The first pathway involves the dissociative migration of the $B(C_6F_5)_3$ unit from one methyl group to the other (eq 10). The second pathway involves the dissociation/recombination of the ion pair (eq 11). Recent

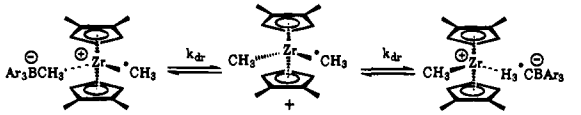

(10)

(11)

solution spectroscopic studies[7e,f] indicate that B—CH_3/M—CH_3 exchange is predominantly if not exclusively $B(C_6F_5)_3$ dissociative in nature (eq 10). For the metallocene ion pair shown, the rate of ion pair reorganization (eq 11) is ~10 times greater than the rate of Zr—Me/B—Me exchange (eq 10) with derived $\Delta G^{\ddagger}$ values being 18.3(2) and 19.7(2) kcal·mol^{-1} at 80 °C, respectively. Although both exchange processes are observed for the methyl cations, anion dissociation/recombination is most relevant to the growing polymer chain disposition during olefin polymerization. Indeed, eq 11 represents insertionless migration, a phenomenon thought to be responsible for the predominant stereochemical defects in syndiospecific propylene polymerization *(vide infra)*.[3]

The thermal instability of the present chiral methyl cations precludes determination of the rate and activation parameters for the analogous exchange processes. However, by studying the temperature dependence of the equilibrium, it was possible to derive ΔH and ΔS for what we assign to be eq 12. The cations derived from the (—)-menthyl metallocenes, (*R*)-**3a** and (*R*)-**3b**, exhibit a marked metal dependence of the equilibrium

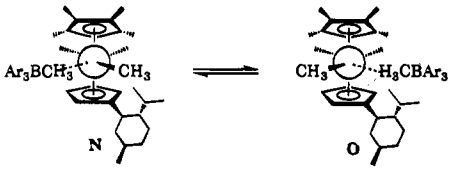

(12)

constant. At 0 °C, the equilibrium constant for the Zr cations is ~0.8 and approaches unity as the temperature is decreased. Surprisingly, the Hf cations have an equilibrium constant of ~0.16 which decreases with decreasing temperature. From plots of ln(K) vs $1/T$, ΔS was determined to be −3.1(1) eu for both the Zr and Hf cations, while ΔH was found to be −0.7(1) and 0.14(3) kcal·mol^{-1}, respectively. Although NOE experiments do not allow unambiguous distinction between major and minor resonances assigned to **N** and **O**, the aforementioned B—Me resonance shift/structure correlation may be used for a tentative assignment. Thus, increasing coordinative unsaturation at the metallocene center correlates with a decrease in the Zr—MeB distance, resulting in a downfield shift of the B—Me resonance. For the present cations, there is a significant chemical shift difference in the two B—Me resonances (~0.25 ppm at 0.0 °C) indicating an appreciable difference in the chemical environment. Assuming that the more deshielded resonance corresponds to the more "tightly" associated ion-pair, structure **N** is assigned to the major isomer in the Zr and Hf (—)-menthyl cations based upon steric considerations. The bulky perfluorotriarylborate anion will likely have greater destabilizing nonbonded contacts with the chiral auxiliary in **O** than in **N**. This argument is supported by the solid state structure of $Cp'_2ZrMe^+MeB(C_6F_5)_3^-$ [7f] which exhibits several close nonbonded contacts between the Cp′ ligands and the aryl groups of the borate anion. These interactions limit the approach of the BMe group to the metal center. The (—)-menthyl chiral auxiliary has substantially more lipophilic bulk than a methyl group (cf., Figures 2 and 3) and should induce even greater steric/energenic differences between **N** and **O**.

Catalytic Olefin Polymerization Mediated by C_1-Symmetric Metallocene Catalysts. General Considerations. Olefin polymerization experiments were carried out at constant temperature in toluene under rigorously anhydrous/anaerobic vacuum line conditions[7f] (see Experimental Section for details). The reactions were quenched after short measured time intervals with acidified methanol followed by polymer collection, washing with pentane, and methanol, and drying *in vacuo* for at least 12 h. The pentane-soluble polypropylene fractions were purified by silica gel chromatography using HPLC grade pentane. In all cases, NMR endgroup analysis indicates that these fractions consist of low molecular weight oligomers.

A. Propylene Polymerization. Several interesting trends are apparent in the propylene polymerization data (Table 3). First, isotacticities can be very high, rivaling or exceeding those of many C_2-symmetric catalysts, with stereoregulation increasing and activity falling with lowering temperature. Furthermore, *there is the marked dependence of catalyst activity and polymer steroregularity/molecular weight on the identity and concentration of the cocatalyst.* Thus, for **2c** + MAO, increasing Al:Zr ratios result in increased activities and molecular weights but in decreased stereoregularity (entries **1**—**7**). Additionally, when Al:Zr ratios of <100 are used, the resulting polymers exhibit very broad molecular weight distributions. Under similar conditions, $B(C_6F_5)_3$ cocatalyzed polymerizations proceed with similar activity and stereoregulation but afford significantly lower polymer molecular weights (entries **8**, **15**, and **16**). Cocatalysts introducing the $B(C_6F_5)_4^-$ counterion exhibit high,

Table 3. Activity, Molecular Weight, and Isotacticity Data for the Polymerization of Propylene by Chiral Organozirconium Complexes

entry	cat[b]	cocat	[cocat][c]	T (°C)	[mon][d]	M_n[e,j]	M_w[e,j]	activity[f]	time (h)	yield[g]	% mmmm[h,j]
1	**2b**	MAO[a]	126	25	0.8	5 180	17 810	8.9×10^4	4.0	5.37/0.05	78
2	**2b**	MAO[a]	126	−5	2.4	8 160	20 390	3.2×10^4	2.0	2.73/0.00	82
3	**2b**	MAO[a]	126	−45	5.0	9 890	23 280	7.8×10^2	2.0	0.14/0.00	93
4	**2b**	MAO[a]	700	25	0.8	1 890	3 460	1.6×10^5	3.0	7.10/2.10	60
5	**2b**	MAO[a]	700	−5	2.4	12 360	25 890	1.3×10^4	2.0	1.10/0.00	75
6	**2b**	MAO[a]	700	−45	5.0	36 950	66 870	2.7×10^3	3.0	0.72/0.00	90
7	**3b**	MAO[a]	700	25	0.8	2 890	6 030	1.7×10^5	3.0	7.46/3.96	82
8	**3b**	$B(C_6F_5)_3$	0.7	25	0.8	1 500	2 400	4.5×10^4	3.0	1.94/0.80	83
9	**3b**	$Ph_3CB(C_6F_5)_4$	0.7	0	1.6	37 800	90 900	1.9×10^5	0.5	2.73/0.00	95
10	**3b**	$HNR_3B(C_6F_5)_4$	0.7	0	1.6	17 700	63 300	1.3×10^5	0.5	1.93/0.00	91
11	**2a**	MAO[a]	700	25	0.8	1 740	2 170	5.4×10^4	3.0	2.32/0.10	35
12	**2a**	MAO[a]	700	−5	2.4	6 750	9 940	2.0×10^4	3.0	2.60/0.05	70
13	**2a**	MAO[a]	700	−45	5.0	8 810	14 230	2.5×10^3	3.0	0.67/0.00	90
14	**3a**	MAO[a]	700	25	0.8	2 850	13 510	4.6×10^4	3.0	2.00/0.15	35
15	**3a**	$B(C_6F_5)_3$	0.7	25	0.8	190[i]		5.4×10^4	3.0	2.34/2.34	
16	**3a**	$B(C_6F_5)_3$	0.7	0	1.6	250[i]		5.4×10^4	3.0	4.70/4.70	
17	**3a**	$Ph_3CB(C_6F_5)_4$	0.7	0	1.6	15 100	31 200	1.6×10^4	0.5	0.23/0.00	64

[a] Methylalumoxane, solvent removed from a 20 wt % solution in toluene (Schering) at 25 °C/10^{-6} Torr. [b] [catalyst] = 0.7 mM in toluene. [c] [co-catalyst], mM in toluene. [d] [monomer], M in toluene. [e] By GPC, relative to polystyrene standards (reproducibility between runs > 15%). [f] Grams total polymer/mol Zr·(mol L^{-1} propylene)·hour (reproducibility between runs > 15 %). [g] Total polymer/pentane-soluble fraction. [h] From pentad analysis in 5/1 v/v 1,2,4-trichlorobenzene/DMSO-d_6 130 °C; delay = 6 s, 45° PW (reproducibility between runs >3 % for large mmmm values). [i] From end-group analysis. [j] Pentane-insoluble fraction.

Table 4. Pentad Distributions in Representative Polypropylenes

entry	mmmm	mmmr	rmmr	mmrr	mmrm + rmrr	mrmr	rrrr	rrrm	mrrm	mmmr:mmrr:mrrm
2	0.8249	0.0538	0.0048	0.0531	0.0224	0.0179	0.0003	0.0004	0.0258	2.06:2.08:1.00
3	0.9436	0.0231	0.0000	0.0221	0.0000	0.0000	0.0000	0.0000	0.0113	1.96:2.04:1.00
5	0.7512	0.0792	0.0035	0.0784	0.0301	0.0179	0.0004	0.0007	0.0386	2.03:2.05:1.00
6	0.9048	0.0310	0.0008	0.0292	0.0146	0.0043	0.0002	0.0003	0.0148	1.97:2.09:1.00
9	0.9451	0.0229	0.0000	0.0214	0.0000	0.0000	0.0000	0.0000	0.0107	2.00:2.14:1.00
10	0.9092	0.0302	0.0013	0.0297	0.0054	0.0100	0.0002	0.0003	0.0137	2.17:2.20:1.00
17	0.6446	0.1141	0.0108	0.1137	0.0455	0.0006	0.0005	0.0131	0.0570	1.99:2.00:1.00

comparable activities and stereoregularities, yielding the highest molecular weights for a given metallocene precatalyst and temperature (entries **9**, **10**, and **17**). It appears that the presence of an exogeneous amine base (entry **9** vs **10**) significantly depresses the molecular weight of the polymer produced under the present polymerization conditions. The above effects are reasonably a consequence of the demonstrated tight, sterically demanding, and differing ion pairing between the various anions and the chiral cationic reaction centers *(vide infra)*.

High isotacticities are observed under certain conditions in the present study, but the molecular weights of the polypropylenes are not exceptionally high. Although no attempt was made to optimize molecular weights in the present experiments, this general behavior is typical of substituted Cp metallocene catalyst systems.[8a,b] Generally, polymer molecular weights increase as the electron donating ability of the π-ancillary ligation increases, and, for example, substituted indenyl ligand systems typically produce polymers with molecular weights $\gtrsim 10x$ those of analogous Cp systems.[1]

Polypropylene Microstructure. Polymer microstructure was characterized by solution $^1H/^{13}C$ NMR according to standard protocols.[1,2] Homosteric sequence analysis at pentad resolution was performed on the polypropylene samples to determine stereoregularities and to obtain information about the polymerization mechanism. However, complete analysis was only performed on samples with sufficiently high molecular weight that intrusive end-group effects were not significant. The microstructure of a polypropylene is represented in **P** including the standard assignments of relative stereochemistry.[50,51] For polypropylene, there are a total of nine resolvable resonances

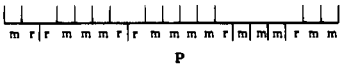

corresponding to 10 possible observable pentads.[2] The relative pentad populations may be used to differentiate between the two basic types of stereocontrol observed in Ziegler–Natta α-olefin polymerization (chain-end-control vs enantiomorphic site-control). The major polymer stereochemical defect produced by the present C_1-symmetric catalysts is isolated racemic triads (m**r**rm, e.g., **Q**), and the population ratio of the mmmr:mmrr:mrrm pentads is consistently ~2:2:1 (Table 4). These observations are consistent with stereoregulation by an enantiomorphic (metal-centered, self-correcting) site-control

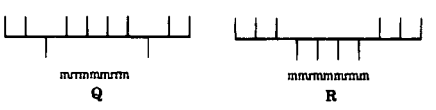

mechanism[2e,50,52] resulting from the designed asymmetry of the metal–ligand–anion templates. Stereoblock polymers of structure **R** would be expected from chain-end-control (Bernoullian) mechanisms. The predominant stereochemical defect in such polymers is isolated racemic diads (mm**r**m), and the ratio of mmmr:mmrm populations is predicted to be 1:1.[2e,50,52] The data in Table 4 are not consistent with this latter model.

The propagation step in Zieler–Natta α-olefin polymerization consists of successive regioregular (1,2) insertions of monomer into the metal–carbon bond of the growing polymer chain (eq 13). One of the characteristic differences in the polymers

(50) Bovey, F. A. *Chain Structure and Conformation of Macromolecules*; Academic: New York, 1982; pp 78–84.

(51) Frisch, H. L.; Mallows, C. L.; Bovey, F. A. *J. Chem. Phys.* **1966**, *45*, 1565–1579.

(52) Shelden, R. A.; Fueno, T.; Tsunetsugu, T.; Furokawa, J. *J. Polym. Sci. Part B* **1965**, *3*, 23–35.

produced by homogeneous and heterogeneous Ziegler–Natta

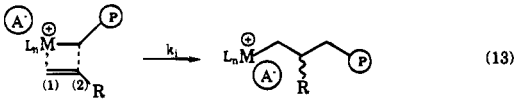

(13)

catalyst systems is the number of regioirregular (2,1) insertions (eq 14).[53] The former catalysts typically produce polymers containing 1–5% regioirregularities, while polymers produced by the latter catalysts typically contain <1% of these irregularities. These regioirregularities are easily identifiable in the

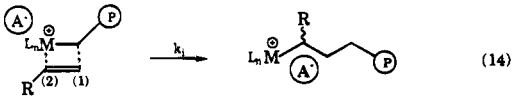

(14)

polypropylene ^{13}C NMR spectrum since the resonances assignable to these segments (**S** and **T**) fall in relatively absorption-free regions of the spectrum.[54] The polymers produced by the present catalysts contain ~1% of these regioiregularities as estimated from the ^{13}C NMR spectra.

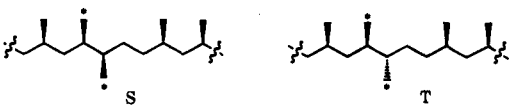

Endgroup analysis provides important insight into chain transfer processes in Ziegler–Natta polymerization. Of the four possible endgroups usually observed (**U**–**X**), only **U** and **V** are observed in the product of the present C_1-symmetric catalytic polymerizations. The presence of *n*-Pr (**U**) and vinylic (**V**) endgroups is consistent with chain transfer exclusively via β-H elimination.[6f,54] Allylic (**W**) and *i*-Pr (**X**) end-groups are usually associated with β-Me elimination.[6f,54c] Additionally, end-group **X** is also thought to arise via chain transfer (Zr-P/Al-Me

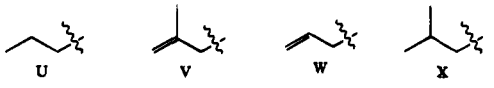

exchange) to Al of MAO co-catalysts.[54c] The **W**/**X** ratio is used to determine the relative contributions of the latter two chain transfer mechanisms. Generally accepted pathways for formation of endgroups **U**–**X** are shown in Scheme 1.

All three of the aforementioned chain transfer pathways have been observed in homogeneous "cationic" metallocene polymerization systems, and the relative contributions of each to overall chain transfer can be correlated with metal ligation structure.[6f,54c] The β-H elimination transition state is sufficiently sterically demanding in regard to C-to-Zr H delivery that it is usually only significant in the case of Cp_2MP^+ catalysts. Conversely, for the more sterically encumbered Cp'_2MP^+ catalysts, β-H elimination is usually not observed, and β-Me elimination is typically the predominant if not exclusive chain transfer process observed above 0 °C.[7f,54c] However, at lower temperatures, chain transfer to aluminum becomes the dominant chain transfer pathway in Cp'_2MP^+–MAO catalyst systems. The observed exclusivity of β-hydride elimination in the present C_1-symmetric catalysts is thus in accord with structure/reactivity patterns observed in typical achiral "cationic" group 4 metallocene systems.

Scheme 1. Chain Transfer Pathways in the Ziegler–Natta Polymerization of α-Olefins

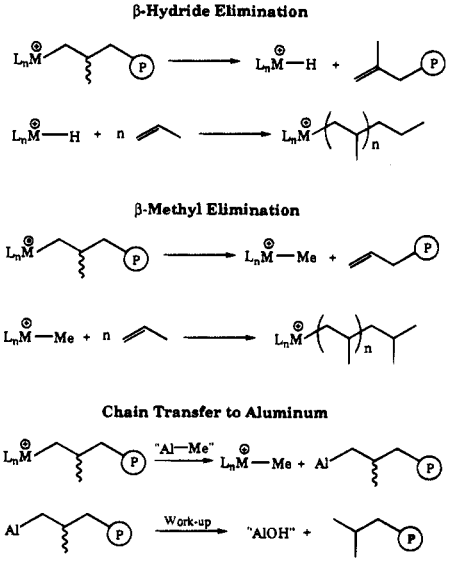

B. Ethylene Polymerization. The polyethylenes produced by the present C_1-symmetric catalysts are of relatively high molecular weight and narrow polydispersity (Table 5). Solution ^{13}C NMR (120 °C in 2,4,6-trichlorobenzene) indicates that all of the polymers are highly linear.[55] The observed catalytic activities are slightly lower than those observed in parent achiral $Cp_2ZrMe^+MeB(C_6F_5)_3^-$ (compare entries **1** and **2**). As with the propylene polymerizations, there is a marked counterion effect on catalyst performance. For a given catalyst and temperature, $B(C_6F_5)_4^-$ produces polymers with higher molecular weights and exhibits higher activities. This effect becomes more pronounced as the reaction temperature is descreased (compare entries **3** and **4**; **6** and **7**, **8**; **9** and **10**). Additionally, for a given cocatalyst and temperature, the Hf derivative exhibits similar activity but produces higher molecular weight polymers (entries **4** and **5**). Furthermore, dramatic differences in activity are observed at low temperature with the Hf derivative, and only traces of polymer are produced at −20 °C (entries **6** and **9**). Finally, the presence of exogeneous amine has only a minor effect on catalyst activity and polyethylene molecular weight (entries **7** and **8**).

Discussion

Catalyst Synthesis. The synthesis of the present C_1-symmetric metallocene dichlorides proceeds in good yield under high dilution conditions. At higher reagent concentrations, significant amounts of an intractable side product are produced. This phenomenon has been noted by others and is probably a major factor in the low (5–25%) yields often reported for other Cp-bridged group 4 metallocenes. Diastereoselectivity in the present complexation reactions is surprisingly insensitive to reaction conditions such as temperature, solvent, anionic ligand counterion, and chiral auxiliary. The product distribution is undoubtedly kinetic in origin with the initially formed products being configurationally stable indefinitely in donor solvents, even at elevated temperatures. Paquette and co-workers have extensively analyzed the π-facial selectivity of group 4 metal addition in a number of annulated Cp systems and have found, without exception, that capture of nucleophilic dienides by MCl_4

(53) Grassi, A.; Zambelli, A.; Resconi, L.; Albizzati, E.; Mazzocchi, R. *Macromolecules* **1988**, *21*, 617–622.

(54) (a) Tsutsui, T.; Mizuno, A.; Kashiwa, N. *Polymer* **1989**, *30*, 428–431. (b) Longo, P.; Grassi, A.; Pellecchia, C.; Zambelli, A. *Macromolecules* **1987**, *20*, 1015–1018. (c) Resconi, L.; Piemontesi, F.; Franciscono, G.; Abis, L.; Fiorani, T. *J. Am. Chem. Soc.* **1992**, *114*, 1025–1032.

(55) (a) Reference 50, pp 78–91. (b) Encyclopedia of Polymer Science; Wiley: New York, 1987; Vol 10, pp 298–299.

Table 5. Activity and Molecular Weight Data for the Polymerization of Ethylene by (*R*)-Me_2SiCp''(−)-menthylCpMMe_2 Complexes[a]

entry	cat, amount	co-cat, amount	temp (°C)	time (s)	PE (g)	activity[b]	M_n[c]	M_w[c]	M_w/M_n
1	.	$Cp_2ZrMe^+MeB(C_6F_5)_3^-$ [d]	25	40	0.65	4.5×10^6	61 200	124 000	2.0
2	**3a**, 10 mg	$B(C_6F_5)_3$, 11 mg	20	90	1.01	3.0×10^6	63 900	103 400	1.6
3	**3a**, 10 mg	$B(C_6F_5)_3$, 11 mg	0	300	0.60	5.4×10^5	94 300	160 500	1.7
4	**3a**, 10 mg	$Ph_3CB(C_6F_5)_4$, 19 mg	0	150	0.84	1.5×10^6	177 100	313 000	1.8
5	**3b**, 12 mg	$Ph_3CB(C_6F_5)_4$; 19 mg	0	60	0.36	1.6×10^6	261 900	441 000	1.7
6	**3a**, 10 mg	$B(C_6F_5)_3$, 11 mg	−20	240	0.13	1.5×10^5	34 800	59 700	1.7
7	**3a**, 10 mg	$Ph_3CB(C_6F_5)_4$, 19 mg	−20	60	0.42	1.9×10^6	251 300	427 200	1.7
8	**3a**, 10 mg	$^nBu_3NHB(C_6F_5)_4$, 18 mg	−20	60	0.33	1.5×10^6	232 500	401 100	1.7
9	**3b**, 12 mg	$B(C_6F_5)_3$, 11 mg	−20	300	trace				
10	**3b**, 12 mg	$Ph_3CB(C_6F_5)_4$, 19 mg	−20	300	0.18	7.9×10^5	322 200	534 300	1.7

[a] Carried out in 50 mL of toluene and at 1 atm ethylene. [b] Gram total polymer/mole metal·atm·h. [c] By GPC, relative to polystyrene standards. [d] 0.32 mM in 40 mL toluene, from ref 7f.

and $[CpH_xR_{5-x}]MCl_3$ moeities is irreversible.[56] However, in these same studies it was found that product distribution (*exo* vs *endo* complexation of bicyclic annulated Cp's) may be greatly influenced by reaction temperature, with the *endo* product being favored at higher temperatures. Brintzinger and co-workers have also examined π-facial selectivity in the formation of a number of heteroannular bridged $X(RR'Cp)_2MCl_2$ (X = Me_2Si or C_2H_2, M = Ti or Zr) *ansa*-metallocenes.[28a-c] Interestingly, the stereochemical distribution of the incipient reaction products (*meso* vs *rac*) is dependent upon the nature of the heteroannular bridge and the counterion of the bis(dieneide) reagent. For Me_2-Si bridges, the product distribution is insensitive to all reaction conditions. However, for the "ethano" bridges, *rac* complexes are highly favored if the counterion is K^+. In the synthesis of related axially- and C_2-symmetric metallocenes, four steps (complexation, separation of *meso* from *rac* isomers, derivatization, and resolution via separation of diastereomers) are required to obtain the homochiral metallocenes. Theoretically, if these steps were quantitative, the maximum yield of a single antipode of a C_2-symmetric metallocene of the above types would be 50%. However, the reported overall yields in the literature range from 4−25%. *In contrast, the (−)-menthyl derivatives of the present C_1-symmetric metallocenes provide a one step, relatively high yield (60−70%) route to the optically pure chiral metallocene, clearly demonstrating an attraction of C_1-symmetric complexes.*

The synthesis of the present metallocene dimethyl complexes proceeds in high yield at ambient temperature. However, an excess of alkylating reagent is required for complete conversion of the metallocene dichloride to the dimethyl complex. The alkylation can be conveniently monitored by ^1H NMR. The first product formed in the alkylation is the metallocene methyl chloride which exhibits a characteristic M−Me resonance at δ 0.2 ppm. In the preparation of the Zr dimethyl complexes, there can be a significant amount of reduction (Zr(IV) → Zr(III)) concurrent with alkylation.[27,33] This is usually not observed in the preparation of the Hf analogs presumably due to the greater difficulty in reducing Hf(IV).[27,33] However, isolated yields in both of the present cases are generally >85%.

Synthesis of active C_1-symmetric polymerization catalysts proceeds smoothly in toluene with short induction periods (1−5 min). Unfortunately, attempts at isolating the chiral metallocene methyl cation salts were unsuccessful due to the thermal lability of the complexes both in solution and in the solid state. However, catalyst solutions maintained below 5 °C remain catalytically active for days. "Cationic" group 4 metallocenes are exceedingly air- and moisture-sensitive and require high vacuum line/glovebox techniques for efficient handling. The use of excess MAO (Al/Zr > 10 000) is necessary for high catalyst activities if rigorous exclusion of air, moisture, and other impurities in the solvent and monomer feed are not maintained.[35] Recently Chien and co-workers have shown that for stoichiometric borate co-catalyzed polymerizations, as much as 96% of the active catalyst is sacrificed to scavenge the aforementioned impurities if scrupulous purification procedures are not employed.[57] For these reasons, extensive precautions were taken to remove impurities in the present study, and reproducibly high polymerization activities were observed (see Experimental Section for details).

Olefin Polymerization. To date, several mechanistic aspects of homogeneous, metallocene-centered stereoregular Ziegler−Natta olefin polymerization have been elucidated. The importance of stabilizing α-agostic interactions in the olefin insertion transition state is supported both experimentally[1,58] and theoretically.[5c] This effect is undoubtedly a result of the extreme electrophilicity/coordinative unsaturation of the "cationic" (14 electron) metallocene. Additionally, the effects of ring substituents α and β to the heteroannular bridge of *ansa*-metallocenes has been extensively investigated.[1,5a] It has been shown that β substituents provide the predominant basis for enantioface discrimination in the stereospecific polymerization of α-olefins. Furthermore, correlations between catalyst structure and the various observed chain transfer pathways have been drawn.[7f,54c] As catalyst electrophilicity increases, there is a concomitant increase in chain transfer rate, resulting in a decrease in the polymer molecular weight. However, a number of important questions remain unanswered. Important solution dynamic processes that occur on the time scale of the polymerization include the disposition of the coordinated monomer, the location and conformation of the growing polymer chain, and the proximity and role of the charge-compensating counteranion. Investigations by Ewen and co-workers on MAO and *N,N*-dimethylanilinium tetraperfluorophenylborate co-catalyzed syndiospecific propylene polymerization using C_s-symmetric metallocenes suggested that the counteranion has little or no effect on catalytic activity or on the microstructure of the resulting polyolefin.[3d] It was concluded that the anion was a "spectator" having little influence on the course of polymerization. In contrast, Chien and co-workers recently reported a comparative study of $MeB(C_6F_5)_3^-$ and $B(C_6F_5)_4^-$ anions with C_2-symmetric ethanobridged bis(indenyl) zirconocene catalysts.[57a] While there is no counterion influence on product molecular weight, there is a marked anion influence on both stereoregulation and catalyst

(56) (a) Paquette, L. A.; Moriarty, K. J.; Meunier, P.; Gautheron, B.; Sornay, C.; Rogers, R. D.; Rheingold, A. L. *Organometallics* **1989**, *8*, 2159−2167. (b) Paquette, L. A.; Moriarty, K. J.; Meunier, P.; Gautheron, B.; Crocq, V. *Organometallics* **1988**, *7*, 1873−1875.

(57) (a) Vizzini, J. C.; Chien, J. C. W.; Babu, G. N.; Newmark, R. A. *J. Polym. Sci. A Polym. Chem.* **1994**, *32*, 2049−2056. (b) Chien, J. C. W.; Song, W.; Rausch, M. D. *J. Polym. Sci. A Polym. Chem.* **1994**, *32*, 2387−2393.

(58) (a) Leclerc, M. K.; Brintzinger, H. H. *J. Am. Chem. Soc.* **1995**, *117*, 1651−1652. (b) Piers, W. E.; Bercaw, J. E. *J. Am. Chem. Soc.* **1990**, *112*, 9406−9407. (c) Krauledat, H.; Brintzinger, H. H. *Angew. Chem., Int. Ed. Engl.* **1990**, *29*, 1412−1413. (d) Clawson, L.; Soto, J.; Buchwald, S. L.; Steigerwald, M. L.; Grubbs, R. H. *J. Am. Chem. Soc.* **1985**, *107*, 3377−3378.

activity. Solvent-dependent polymerization effects also suggest a significant role for the "tightness" of the cation-anion pairing.[57b,59] The results of the present studies with C_1-symmetric metallocenes and the aforementioned mechanistic questions form the basis for the following discussion. Significant counterion effects on polymer molecular weight are discussed first followed by a discussion of factors influencing polymer microstructure.

Catalyst Effects on Polymer Molecular Weight. The two well-defined counterions, $MeB(C_6F_5)_3^-$ and $B(C_6F_5)_4^-$, used in the present polymerization studies produce dramatically different polymers. The molecular weights of the polymers produced by the respective catalysts under identical reaction conditions differ by >10× for propylene polymerization (Table 3 entries **8,9** and **16,17**) and up to 8× in ethylene polymerization (Table 5 entries **3,4** and **6,7**). ^{13}C NMR spectra of the polymeric products indicate that β-hydride elimination is the only significant chain transfer pathway. Therefore, the molecular weight of the polymer is controlled by the relative rates of two competing processes, β-hydride elimination and olefin insertion. For propylene polymerization, the overall number of insertions (based on activity) is approximately equal for both anions. Therefore, large anion-sensitive disparities in $k_{\beta\text{-hydride}}$ elimination must be responsible for the marked molecular weight differences. For the polymerization of less sterically demanding ethylene, both polymer molecular weight and catalyst activity are higher for $B(C_6F_5)_4^-$ than for $MeB(C_6F_5)_3^-$. This effect reasonably reflects disparities in both $k_{\text{insertion}}$ and $k_{\beta\text{-hydride}}$ elimination.

If the anion and cation exist as a tight ion pair (Scheme 2, (**1**)), and generation of a free/less encumbered cation (**2**) is necessary to either bind and activate olefin or for β-hydride elimination (approximately the microscopic reverse), then the "tightness" of the ion pair and the attendant local steric congestion should strongly influence the rates of these processes. For achiral $L_2ZrMe^+MeB(C_6F_5)_3$ (L = Me_5C_5, 1,2-$Me_2C_5H_3$, and C_5H_5) systems only slight diffraction-determined differences in the separation of the anion and cation manifest themselves in significant reactivity differences.[7f] Interestingly, ethylene polymerization is most rapid for the L = C_5Me_5 catalyst in which the anion is more loosely bound. This trend reverses, however, for more sterically encumbered propylene.[7f] In the present propylene polymerization studies, the presence of an amine base depresses catalytic activity and the molecular weight of the resulting polymer by a factor of ~2. For ethylene polymerization, this effect is less. These results suggest that the amine base may more effectively compete with bulkier propylene for the vacant coordination site of the dissociated ion pair (Scheme 2).

Origin of Stereoselectivity. Two basic models are used to explain induction of stereoregularity in poly-α-olefins produced by homogeneous Ziegler–Natta catalysts such as the present systems. Achiral catalysts can produce stereoblock polymers via chain-end-control,[50] while chiral catalysts generally produce polymers with isotactic microstructure via enantiomorphic site-control.[52] In some cases, the combined effects determine polymer microstructure.[1,60] The asymmetry of the present catalysts as well as the formation of isotactic polymers with isolated racemic triads (mrrm, e.g., **Q**) and mmmr:mmrr:mrrm pentad ratios ~2:2:1 (Table 4) indicate that enantiomorphic site-control plays a major role in stereoregulation.[1,52] High monomer enantioface selectivity argues that the chiral auxiliary effectively shields one side of the metallocene from incoming monomer. High enantioface selectivity is observed in a number of other catalytic processes involving this C_1-symmetric ligation array.[11b-d]

Although no d° metallocene complexes with exogenous olefins have yet been isolated,[61] it is reasonable to assume that monomer is coordinated to/activated by the metal center prior to insertion. Furthermore, Ewen's studies of syndiospecific propylene polymerization by C_s-symmetric metallocenes suggest that alternating site migratory olefin insertion (eq 15) is responsible for the predominant rrrr pentad distribution (**AA**) in the resulting polyolefin.[1,3] These results indicate that

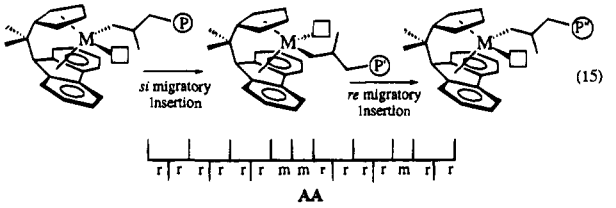

(15)

insertionless migration (site isomerization without olefin insertion, e.g., eqs 11 and 16) of the growing polymer chain does not effectively compete with olefin binding/activation and

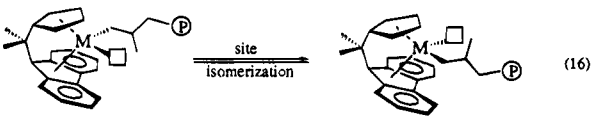

(16)

subsequent insertion. The observed counterion ($B(C_6F_5)_4^-$ vs MAO^-) independence[3d] of catalyst activity and polymer microstructure in this case suggests that these counterions are equally coordinating/intruding and do not introduce substantially different steric constraints on the coordinated monomer orientation.

For typical C_2-symmetric catalysts, insertionless migration should not, in principle, introduce stereochemical defects in the predicted isotactic polymer microstructure since both metallocene activation sites select for the same monomer enantioface (**BB**). Ignoring the role of counteranion, the inherent enantioface selectivity of these catalysts should then be the predominant factor controlling polymer stereoregularity. However, as noted

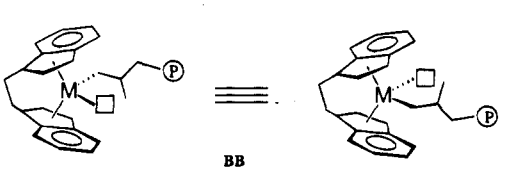

Scheme 2. Possible Mechanism for Olefin Polymerization Mediated by Chiral C_1-Symmetric Organo-Group 4 Complexes

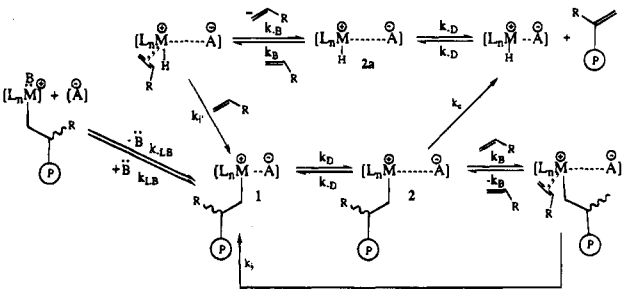

$k_i \approx k_{i'}$ = rate constant for olefin insertion[a]
k_e = rate constant for β-hydride elimination
k_D = rate constant for anion/cation dissociation
k_{LB} = rate constant for Lewis base binding
k_B = rate constant for olefin binding

[a] $^a k_i$ (insertion into M–H) is probably larger than k_i (insertion into polymer chain) based on steric considerations.

(59) Herfert, N.; Fink, G. *Makromol. Chem.* **1992**, *193*, 773–778.
(60) Masamune, S.; Choy, W.; Petersen, J. S.; Sita, L. R. *Angew. Chem., Int. Ed. Engl.* **1985**, *24*, 1–76.
(61) (a) For the spectroscopic detection of organolanthanide-exogenous olefin complexes, see: Nolan, S. P.; Marks, T. J. *J. Am. Chem. Soc.* **1989**, *111*, 8538–8540. (b) For d° complexes of "tethered" olefins, see: Jordan, R. F.; Wu, Z.; Petersen, J. L. *J. Am. Chem. Soc.* **1995**, *117*, 5867–5868. Casey, C. P.; Hallenbeck, S. L.; Pollock, D. W.; Landis, C. R. *Abstracts, 210th ACS National Meeting*; Chicago, IL, Aug 1995, INOR 28.

Scheme 3. Proposed Mechanism for Propylene Polymerization Mediated by C_1-Symmetric Metallocenes (1)

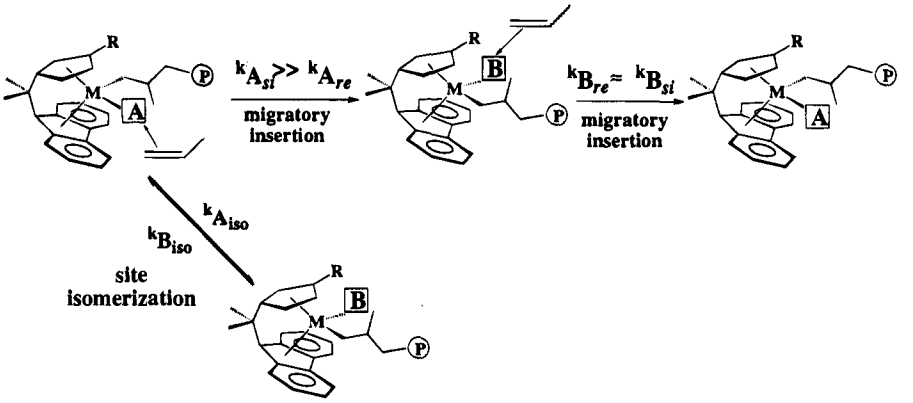

above, Chien and co-workers recently reported significant counterion identity and solvent polarity effects on polymerization activity and on polymer stereoregularity/molecular weight.[57] Additionally, Brintzinger and co-workers have recently proposed a chain-end isomerization process which proceeds via intramolecular σ-bond metathesis (e.g., eq 17).[58a] This process, if competitive with intramolecular olefin binding/insertion, may be responsible for instances of stereoregulation which are dependent upon monomer concentration.[3d,8c,62]

A priori, C_1-symmetric metallocenes (**CC**) could produce polymers with a range of microstructures depending on the relative rates of olefin insertion (k_{re} and k_{si} for each site) and polymer-chain site isomerization (cf., **A** ⇌ **B**, in **CC** and eqs 11 and 16). The following discussion will consider three

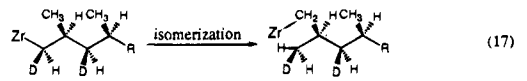

(17)

limiting cases. The first two involve known catalyst systems and the third is a model of the present C_1-symmetric catalysts.

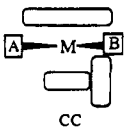

CC

C_1-symmetric metallocene **DD** was developed by Ewen and co-workers[2c] and is a methylated derivative of the C_s-symmetric metallocene described previously (**E**, eq 15). The addition of the methyl group on the Cp β to the bridge renders activation/insertion sites **A** and **B** inequivalent. The polymer produced by this catalyst/MAO system is hemiisotactic[63] (**EE**). In this and following representations of polymer microstructure, **A** and **B** denote which activation site is responsible for the observed

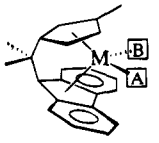

DD

EE

stereochemistry. This polymer has a microstructure consisting of alternating stereospecific and stereorandom methyl attachment. If chain growth occurs through the migratory insertion mechanism proposed for the parent C_s-symmetric metallocene, then addition of the methyl Cp substituent renders one of the activation/insertion sites stereorandom. Based on ligand steric arguments, site **B** would most likely be aspecific ($^kB_{re} \approx {}^kB_{si}$) due to unfavorable nonbonding interactions between the incoming monomer methyl group and the β-methyl substituent of the Cp moiety.[1] Additionally, the alternating microstructure implies that insertionless migration (eqs 11 and 16) does not effectively compete with olefin binding and subsequent insertion. This lack of competitive site isomerization can be attributed to either of two scenarios. Either the rate of olefin insertion is rapid compared to the rate of isomerization ($^kA_{re}$, $^kA_{si}$, $^kB_{si} \gg {}^kA_{iso}$, $^kB_{iso}$), or the isomerization is rapid but lies in the direction of the inserted product. This later phenomenon could be attributed to conformational effects of the stereocenter created by the previously inserted unit (chain end-control). This mechanistic scenario is illustrated in Scheme 3. Interestingly, increasing the bulk of the Cp β substituent from methyl to *tert*-butyl produces isotactic polypropylene (vide infra).[64]

The second C_1-symmetric catalyst to be considered was reported by Chien and co-workers[4b,c] (structure **FF**). The M = Zr/MAO system exhibits low activity for production of hemiisotactic polypropylene (**EE**).[65] However, when M = Ti, a thermoplastic-elastomer is formed.[4b,c] This rheological behavior

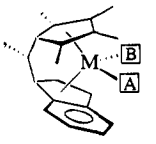

FF

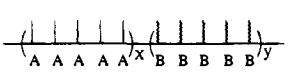

GG

and polymer pentad distribution were attributed to stereoblock microstructure **GG** consisting of stereoblocks less than 20 units each. The blocks attributed to site **A** are stereoregular (forming crystalline regions), while the blocks attributed to site **B** are stereoirregular (forming amorphous regions). The M = Zr scenario is the same as observed for catalyst structure **DD** (Scheme 3). The M = Ti scenario is not consistent with any previous combination of rate and equilibrium constants. However, a scenario that would produce a similar polymer microstructure is illustrated in Scheme 4. Here, the rate of site isomerization is similar to the rates of olefin insertion with site **B** stereospecific and site **A** aspecific. The resulting polymer would have microstructure **HH**. The differences in insertion rates (k_A and k_B) and the site isomerization rates would then account for the block structure and the block dimensions. A

(62) Rieger, B.; Jany, G.; Fawzi, R.; Steimann, M. *Organometallics* **1994**, *13*, 647–653.

(63) (a) Farina, M. *Top. Stereochem.* **1987**, *17*, 18–42. (b) Di Silvestro, G.; Sozzani, P.; Savare, B.; Farina, M. *Macromolecules* **1985**, *18*, 928–932. (c) Farina, M. Di Silvestro, G.; Sozzani, P. *Macromolecules* **1982**, *15*, 1451–1452.

(64) (a) Ewen, J. A.; Elder, M. J. Eur. Pat. Appl. 1993 EP-A 0537130. (b) *Ziegler Catalysis*; Fink, G., Mülhaupt, R., Brintzinger, H. H., Eds.; Springer: Berlin, 1995. (c) *Synthetic, Structural and Industrial Aspects of Stereochemistry Polymerization*; Tritto, I., Giannini Y., Eds.; *Makromol. Chem. Macromol. Symp.* **1995**, *89*.

(65) Llinas, G. H.; Day, R. O.; Rausch, M. D.; Chien, J. C. W. *Organometallics* **1993**, *12*, 1283–1288.

Scheme 4. Proposed Mechanism for Propylene Polymerization Mediated by C_1-Symmetric Metallocenes (2)

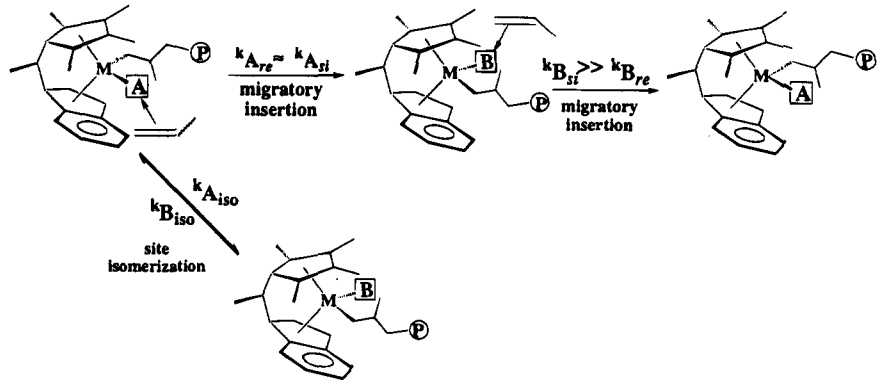

statistical model recently proposed by Collins and co-workers supports this picture.[66]

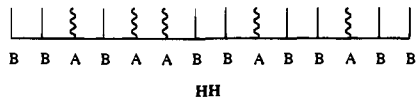

The final C_1-symmetric catalyst structure to be considered is that of the present study (**II**). These catalysts produce isotactic polypropylene (**Q**) with a microstructure and pentad distribution

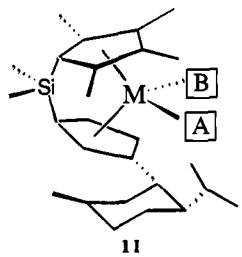

II

consistent with enantiomorphic site-control *(vide supra)*. This microstructure may result from either of two mechanistic scenarios. First, the catalyst may behave like a C_2-metallocene with both **A** and **B** sites selecting for the same monomer enantioface. This scenario seems unlikely because the approach and binding of monomer to site **A** would incur unfavorable steric interactions between monomer methyl group and either Cp methyl groups or the chiral auxilliary (cf., Figure 3). These steric interactions should render site **A** aspecific (if populated), and if chain propagation proceeded through migratory insertion, then a polymer with hemiisotactic microstructure would be expected. However, this is not the case. A more reasonable mechanistic scenario that accounts for the observed polymer microstructure is illustrated in Scheme 5. In this scenario, site **B** is stereospecific, and the rate of site isomerization (**A** ⇌ **B**) is greater than the insertion rate at site **A** ($^kA_{re}$ or $^kA_{si}$). Additionally, the site isomerization rate from **B** to **A** must be small relative to $k_{insertion}$ at site **B**. Either this kinetically disfavored isomerization process or inherent differences in $^kB_{re}$ or $^kB_{si}$ are responsible for stereoerrors in the resulting polymer. It is conceivable that processes such as that depicted in eq 17[58a] may also contribute to stereoerrors.

Conclusions

Chiral C_1-symmetric Zr and Hf complexes of the novel, chelating, cyclopentadienyl-based, $Me_2SiCp''(R^*Cp)$ ancillary ligand have been synthesized. The diastereoselectivity in the initial synthetic complexation reaction is found to be insensitive to reaction conditions and chiral auxiliary. For the (−)-menthyl derivatives, optically pure metallocene may be isolated in good yield after a single recrystallization of the initial complexation and alkylation reaction products. However, the (+)-neomenthyl derivative has only been isolated as a pseudoracemate due to cocrystallization of both the *(R)* and *(S)* isomers in the same crystal lattice. The metallocenes are found to be configurationally stable in donor solvents at ambient and elevated temperatures. Active polymerization catalysts are prepared by reaction of the various metallocenes with a variety of cocatalysts. For propylene polymerization, relatively high isotacticities (>95% mmmm pentad content) are observed, which rival or exceed those of many axially- and C_2-symmetric catalyst systems. Significantly, polymer isotacticities and molecular weight have been found to depend markedly on the quantity and structure of the cocatalyst. Further, these ion-pairing effects offer additional means to modulate polymer stereoregularity and molecular weight. These results clearly demonstrate the competence of C_1-symmetric catalysts in the stereoregular polymerization of propylene and by inference, in other cognate asymmetric transformations.

Scheme 5. Proposed Mechanism for Propylene Polymerization Mediated by C_1-Symmetric Metallocenes (3)

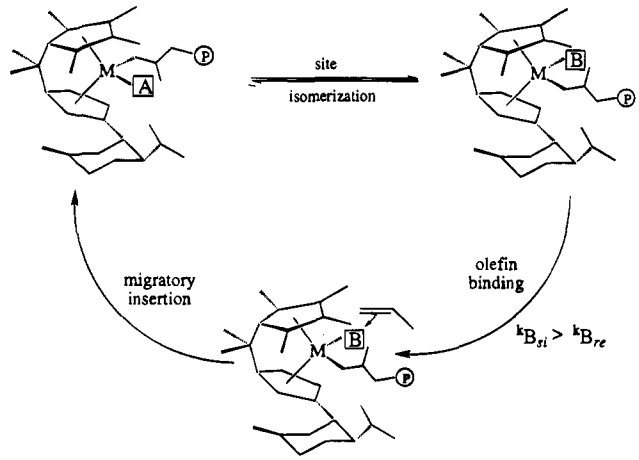

Acknowledgment. This research was supported by the NSF via grant CHE9104112 and by DOE via grant DE-FG02-86ER13511. M.S.E. and M.A.G. thank the Weizmann Institute and Akzo Corp. for postdoctoral and predoctoral fellowships, respectively. We thank Dr. G. M. Smith for Akzo Chemicals for GPC analyses and Professor Paul Loach for access to his CD spectrometer.

Supporting Information Available: Complete tables of positional and anisotropic thermal parameters and full tables of bond distances and angles for *(R)*-**2a** and *(R)*-**3a** (20 pages). This material is contained in many libraries on microfiche, immediately follows this article in the microfilm version of the journal, can be ordered from the ACS, and can be downloaded from the Internet; see any current masthead page for ordering information and Internet access instructions.

JA9516266

(66) Gauthier, W. J.; Collins, S. *Macromolecules* **1995**, *28*, 3779−3786.